

1 **Title: “Late Bayesian inference in sensorimotor behavior”**

2

3 **Evan Remington¹, Mehrdad Jazayeri¹**

4

5 ¹Department of Brain & Cognitive Sciences, McGovern Institute for Brain Research, Massachusetts
6 Institute of Technology, Cambridge, Massachusetts 02139, USA

7

8

9 **Correspondence**

10

11 Mehrdad Jazayeri, Ph.D.

12

13 Robert A. Swanson Career Development Professor

14 Assistant Professor, Department of Brain and Cognitive Sciences

15 Investigator, McGovern Institute for Brain Research

16 Investigator, Center for Sensorimotor Neural Engineering

17 MIT 46-6041

18 43 Vassar Street

19 Cambridge, MA 02139, USA

20 Phone: 617-715-5418

21 Fax: 617-253-5659

22 Email: mjaz@mit.edu

23

24 **Acknowledgements**

25 We would like to thank Josh McDermott, Seth Egger, and Devika Narain for valuable comments

26 regarding the manuscript. M.J. is supported by NIH (NINDS-NS078127), the Sloan Foundation, the

27 Klingenstein Foundation, the Simons Foundation, the Center for Sensorimotor Neural Engineering, and

28 the McGovern Institute.

29 **Abstract**

30
31 Sensorimotor skills rely on performing noisy sensorimotor computations on noisy sensory
32 measurements. Bayesian models suggest that humans compensate for measurement noise and
33 reduce behavioral variability by biasing perception toward prior expectations. Whether the same holds
34 for noise in sensorimotor computations is not known. Testing human subjects in tasks with different
35 levels of sensorimotor complexity, we found a similar bias-variance tradeoff associated with increased
36 sensorimotor noise. This result was accurately captured by a model which implements Bayesian
37 inference after – not before – sensorimotor transformation. These results indicate that humans perform
38 “late inference” downstream of sensorimotor computations rather than, or in addition to, “early
39 inference” in the perceptual domain. The brain thus possesses internal models of noise in both sensory
40 measurements and sensorimotor computations.

41 **Introduction**

42
43 Consider the challenging task of returning a tennis serve. Not only must one accurately infer the path of
44 the ball but also quickly transform that information into a motor plan that would yield a desirable
45 outcome. The ability to apply such transformations is central to our behavioral repertoire and to the
46 performance of athletes, musicians, and professionals such as surgeons and airplane pilots. It has
47 been demonstrated that sensorimotor transformations are noisy (Soechting and Flanders 1989b; Pine
48 et al. 1996; Gordon, Ghilardi, and Ghez 1994; McIntyre et al. 2000; Sober and Sabes 2005;
49 Churchland, Afshar, and Shenoy 2006; Schlicht and Schrater 2007). The ubiquitous nature of
50 sensorimotor transformations in behavior raises an important and unresolved question: does the brain
51 have an internal model of sensorimotor noise (SMN), and do humans adopt strategies to mitigate its
52 effects?

53
54 Research in the past several decades has tackled a similar question in the domain of sensory and
55 motor systems, asking whether the brain is optimized to handle sensory and motor noise. Bayesian
56 models have shown that humans adopt a number of strategies to minimize the effect of sensory and
57 motor noise on behavior. For instance, when multiple sensory cues are available, humans rely more
58 heavily on cues that are more reliable (R. J. van Beers, Sittig, and Gon 1999; Ernst and Banks 2002;
59 Alais and Burr 2004; Bresciani, Dammeier, and Ernst 2008). Similarly, humans use their prior
60 knowledge of statistics of sensory inputs to improve sensory estimates (Weiss, Simoncelli, and Adelson
61 2002; Körding and Wolpert 2004; Tassinari, Hudson, and Landy 2006; Jazayeri and Shadlen 2010).
62 Optimal strategies in the presence of motor noise have also been reported, for example, when some
63 movements are made more costly than others (Trommershäuser et al. 2005; Landy, Trommershäuser,
64 and Daw 2012). These and related observations in multiple modalities (Battaglia, Jacobs, and Aslin

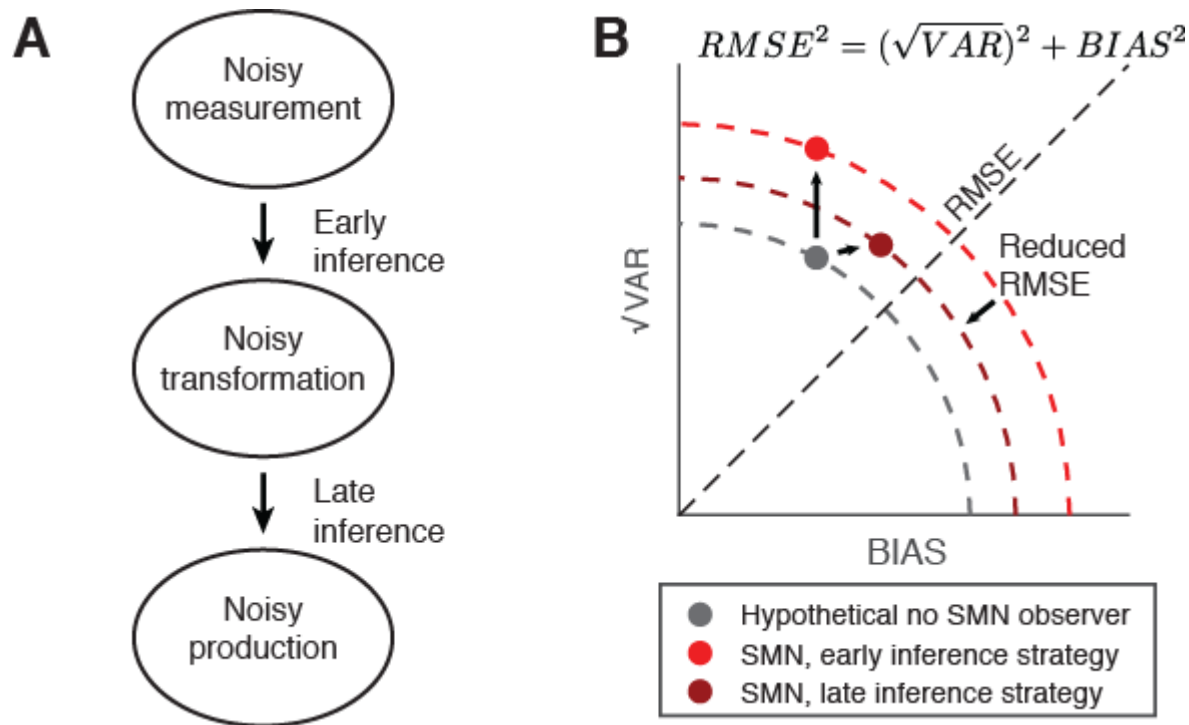
65 2003; Körding, Ku, and Wolpert 2004; Schlicht and Schrater 2007; Burge, Ernst, and Banks 2008;
66 Butler et al. 2010) have provided strong evidence that the brain has an internal model of noisy
67 representations in the sensory and motor systems and implements strategies to reduce their degrading
68 effect on behavior.

69
70 Motivated by the success of normative models showing that the brain seeks to optimize behavior in the
71 presence of sensory and motor noise, we hypothesized that the brain might additionally be equipped
72 with mechanisms to minimize the effects of additional noise introduced by the transformation of sensory
73 inputs to motor outputs (i.e., SMN). This question is particularly important as it bears on where in the
74 brain Bayesian inferences are made (**Figure 1**). Since existing evidence supports perceptual Bayesian
75 inference in the sensory domain (Weiss, Simoncelli, and Adelson 2002; Kersten, Mamassian, and
76 Yuille 2004; Girshick, Landy, and Simoncelli 2011), an observation that Bayesian estimation does not
77 take SMN into account would support the notion that observers employ an “early inference” strategy in
78 which the inference is made within the sensory system before a sensorimotor transformation is applied.
79 If, on the other hand, the brain takes SMN into account, we would conclude that the inference is made
80 downstream after the sensorimotor transformation stage, thus providing evidence for a “late inference”
81 strategy in the association and/or premotor brain areas. Critically, the early and late inference strategies
82 make distinct predictions about the effect of SMN on behavior. With an early inference strategy, any
83 increases in SMN would lead to comparable increases in behavioral variability. In contrast, in the late
84 inference model, the brain would counter this variance by using knowledge about the distribution of
85 responses (i.e., prior distribution). This strategy would introduce additional biases toward the mean of
86 the prior distribution and lead to an overall improvement in performance.

87
88 To distinguish between the early and late inference strategies, we exploited the observation that more
89 complex sensorimotor transformations engender more noise (Soechting and Flanders 1989b; Pine et
90 al. 1996; McIntyre et al. 2000; Sober and Sabes 2005; Schlicht and Schrater 2007). We devised two
91 experiments: (1) a time interval estimation and production task, and (2) a length estimation and
92 production task. In each task, we compared subject’s performance across two sensorimotor contexts.
93 In one context, which we refer to as the “identity context”, the produced quantity (time interval or length)
94 had to match a previously measured quantity. This was compared to a more complex “remapped
95 context” in which subjects had to produce a quantity by applying a non-identity transformation to the
96 sensory quantity. For example, subjects had to produce a length that was 50% longer than the
97 stimulus.

98
99 As expected, the remapped context negatively impacted performance in both tasks, revealing the
100 degrading effect of SMN. Importantly, increases in SMN in the remapped context led to increased
101 biases toward the mean of the sensorimotor prior, an indication of the late Bayesian inference that

102 takes SMN into account. These results reveal that the brain has an internal model of the noise
103 associated with sensorimotor transformations and integrates this information with prior knowledge to
104 optimize inferences in terms of produced quantities.



105
 106
 107 **Figure 1.** Bayesian inference in the presence of sensorimotor noise (SMN). **A.** A schematic of a
 108 sensorimotor task comprising sensory measurement, sensorimotor transformation, and motor
 109 production, all subject to internal noise. In sensorimotor tasks which don't explicitly model SMN,
 110 subjects' behavior is consistent with a strategy in which the effect of sensory noise ("noisy
 111 measurement") on behavior is mitigated by Bayesian inference which biases perceptual estimates
 112 towards the mean of a sensory prior, reducing behavioral variability. We refer to this strategy as "early
 113 inference." An alternate strategy, which we term "late inference" incorporates a prior on behavioral
 114 responses to mitigate the effects of both sensory and sensorimotor noise ("noisy transformation").
 115 Motor noise ("noisy production"), such as that inherent in motor neurons and muscles, cannot be
 116 mitigated by relying on prior information. **(B)** An illustration of relationship between overall variability
 117 (\sqrt{VAR}), overall bias ($BIAS$), and $RMSE$ for the early Inference and late Inference strategies in the
 118 presence of SMN. The equation shows the mathematical relationship between \sqrt{VAR} , $BIAS$, and
 119 $RMSE$. This relationship can be depicted on a quarter circle (dashed lines) with the radius representing
 120 $RMSE$. The gray circle represents \sqrt{VAR} and $BIAS$ values for hypothetical observer with sensory and
 121 motor noise only, and no sensorimotor noise ("no SMN observer"). For this case, early inference and
 122 late inference strategies produce identical behavior (gray). Introducing SMN will cause $RMSE$ to
 123 increase. For an observer that uses an early inference strategy, the increase in $RMSE$ will manifest
 124 primarily as increased \sqrt{VAR} (bright red). In contrast, the effect of SMN in an observer using a late
 125 inference strategy (dark red) would be primarily an increase in $BIAS$. Crucially, the late inference
 126 strategy would lead to a smaller increase in $RMSE$, as represented by the smaller radius of the dark
 127 circle compared to the bright one.

128 **Results**

129
130 We conducted two psychophysical experiments, one involving measurement and production time
131 intervals, and another involving measurement and production of lengths. Each trial in each task
132 consisted of two epochs: a measurement epoch during which a sensory quantity (time interval or
133 length) was measured, and a subsequent production epoch during which subjects had to produce a
134 quantity based on the preceding measurement. For each task, performance was quantified in two
135 sensorimotor contexts: an identity context in which the produced quantity had to match the sensory
136 quantity, and a remapped context in which the produced quantity had to match the sensory quantity
137 multiplied by a fixed scale factor.

138

139 **Time measurement and production task: Ready, Set, Go**

140 Eight human subjects performed a time interval measurement and production task (**figure 2A**), also
141 known as the “Ready, Set, Go” task, similar to a previous study (Jazayeri and Shadlen 2010). During
142 the measurement epoch, subjects were presented with a sample interval (t_s ; see **Table 1** for all
143 variables and abbreviations) demarcated by two visual flashes, “Ready” and “Set” (**figure 2A**). Subjects
144 had to measure t_s and produce an interval (t_p) afterwards by a key press (“Go” - no flash). The interval
145 t_p was measured from the start of the Set flash until the key press. In both identity and remapped
146 contexts, t_s was drawn from the same discrete uniform prior distribution with 11 values ranging from
147 600 and 1000 ms. In the identity context, the correct interval (t_c) was the same as t_s , and in the
148 remapped context, t_c was 1.5 times t_s . In other words, the two contexts were identical during the
149 measurement epochs but differed with respect to the production epoch. We denote these two contexts
150 in terms of a gain factors relating t_c to t_s : gain = 1 for the identity context, and gain = 1.5 for the
151 remapped context. Subjects received trial-by-trial feedback about their performance (see Methods).

152

153 We quantified performance with three statistics (Jazayeri and Shadlen 2010): *BIAS*, which summarizes
154 the deviation of average responses from the correct interval, \sqrt{VAR} , which summarizes the variability of
155 responses across t_s , and *RMSE*, which summarizes the total root mean square error. The three
156 quantities are related through a sum of squares: $RMSE^2 = (\sqrt{VAR})^2 + BIAS^2$ (**Figure 1B**). To ensure
157 that the results were not influenced by overall tendencies to be late or early for all intervals, we
158 calculated these statistics after removing an offset term that accounted for subjects’ overall bias (see
159 Methods). For most subjects, the offset term was relatively small (**see Supplementary Table 1**).

160

161 **Figure 2B** illustrates the behavior of a typical subject in the identity (gray) and remapped (red) contexts
162 of the timing task. Subjects’ behavior in the identity context exhibited prior-dependent bias, consistent
163 with Bayesian integration as was shown previously (Jazayeri and Shadlen 2010; Acerbi, Wolpert, and
164 Vijayakumar 2012; Cicchini et al. 2012) (**figure 2B**, in gray). In the remapped context, subjects had to
165 perform the same task but with a gain of 1.5. We hypothesized that this more challenging sensorimotor

166 transformation would cause an increase in SMN, and would thus increase the total *RMSE*. Additionally,
167 we hypothesized that the increase in *RMSE* would be predominantly due to an increase in bias,
168 consistent with the late inference hypothesis.

169
170 We tested the first hypothesis (increased SMN in the remapped context) by comparing behavior in the
171 remapped context to that predicted under the assumption of no additional SMN. This null hypothesis
172 can be formulated straightforwardly by applying the gain factor of 1.5 to the estimates of t_s and taking
173 into account the additional variability in t_p due to the linear scaling of production noise (Rakitin et al.
174 1998; Gallistel and Gibbon 2000). This leads to a simple prediction: without additional SMN, *RMSE*,
175 *BIAS*, and \sqrt{VAR} in the remapped context should be 1.5 times their values in the identity context (**figure**
176 **2B,C**). As shown by the example subject (**figure 2C**) as well as results across all eight subjects (**figure**
177 **3A, top**), the observed *RMSE* in the remapped context was consistently and significantly higher than
178 expected under the assumption of no additional SMN (*RMSE* median = 130 ms, interquartile range =
179 20 ms vs. median = 180 ms, IQR = 40 ms, $p = 0.016$, Wilcoxon signed-rank test). This provides direct
180 evidence that SMN increased in the remapped context and validates the success of our experimental
181 design in manipulating SMN independently of sensory noise.

182
183 Having established an increase in SMN in the remapped context, we tackled the second hypothesis of
184 whether the *RMSE* increase was due to an increased bias, as would be predicted if subjects optimized
185 their behavior to mitigate the effect of SMN with the late inference strategy. The null hypothesis, which
186 states that subjects do not optimize their behavior in the presence of SMN, can be formulated by an
187 early inference strategy. In this strategy, subjects take the sensory noise into account but ignore SMN.
188 This early inference strategy predicts that the increase in *RMSE* in the remapped context should be
189 explained by an increase in \sqrt{VAR} and not *BIAS*. This is because, in the early inference strategy, SMN
190 is introduced after the inference stage and thus can only lead to increased variance (see **Figure 1B**).
191 As shown in **Figure 2C** for one example subject, the increase in *RMSE* was largely due to an increase
192 in *BIAS*, which can be readily seen as an excess bias compared to the no additional SMN prediction
193 (**Figure 2B, Excess bias**). The results for all subjects, summarized in **Figure 3A**, indicate a clear
194 increase in the *BIAS* for the remapped context relative to the null prediction (*BIAS* median = 73 ms,
195 interquartile range (IQR) = 30 ms vs. median = 130 ms, $p = 0.023$). Across subjects, there was also a
196 small but consistent effect on \sqrt{VAR} (median = 106 ms, IQR = 15 ms vs. median = 113 ms, IQR = 28 ms,
197 $p = 0.008$). *RMSE*, *BIAS*, and \sqrt{VAR} for individual subjects are summarized in **Supplementary Table 1**.
198 The substantial increase in *BIAS* across subjects rejects the null hypothesis and provides evidence for
199 the late Bayesian inference, and indicates that humans take SMN into account to optimize their
200 responses.

201
202 Next, we compared the behavior of subjects in the two contexts using a Bayesian observer model

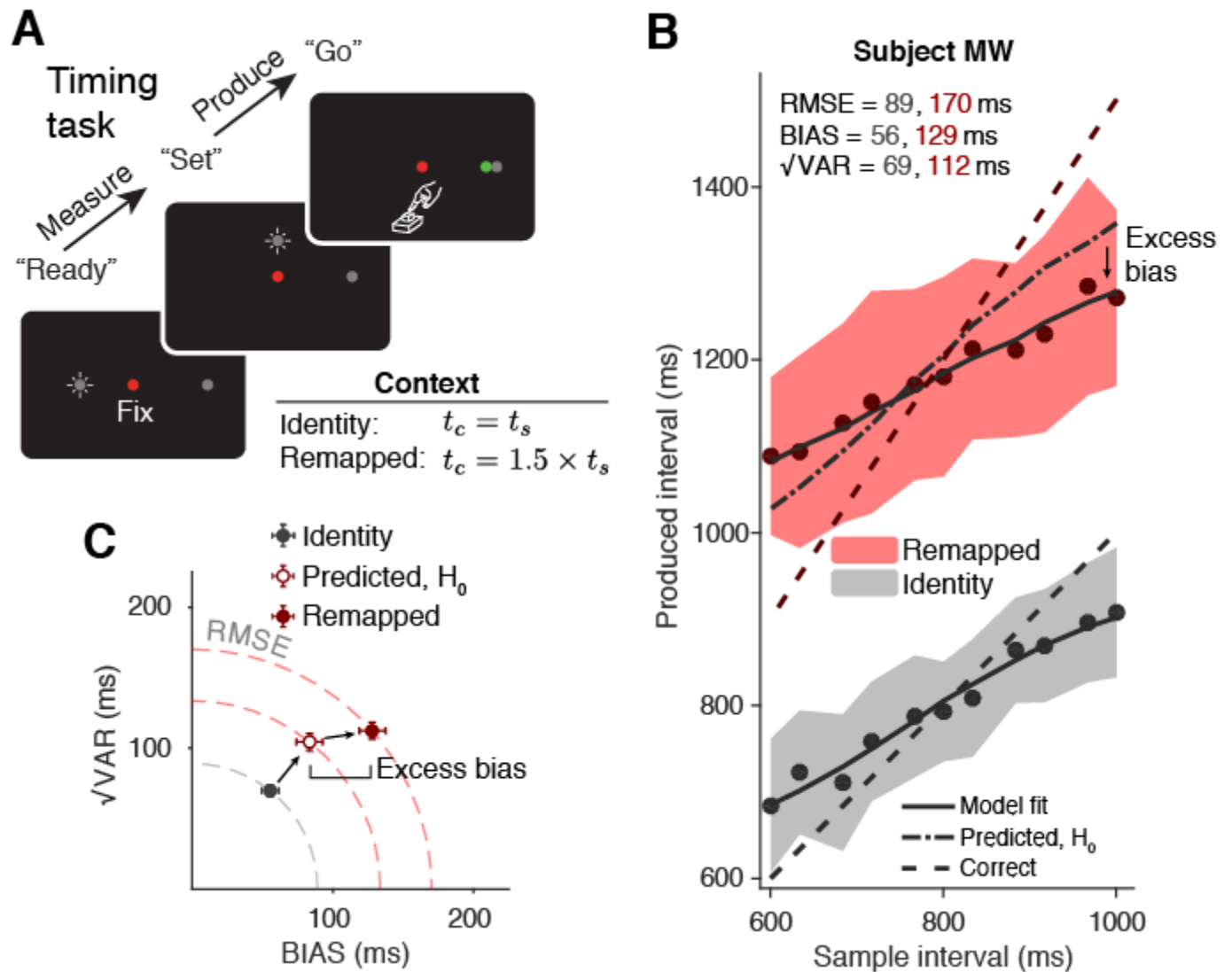
203 **(Supplementary Figure 1**; Equation 4). This model comprises a noisy measurement stage (with scalar
204 noise parameterized by w_m), followed by a Bayesian estimation stage (Bayes-Least Squares), followed
205 by a noisy production stage (with scalar noise parameter w_p) (Jazayeri and Shadlen 2010). The model
206 established Bayes-optimal behavior in the identity context (**Figure 2B**, “model fit,” bottom). We then fit
207 the same model to subjects’ data in the remapped context allowing the parameters (w_m and w_p) to take
208 different values (**Figure 2B**, “model fit,” bottom). Without a mechanism to take SMN into account
209 explicitly, the fits of this model to the remapped context would misattribute the drop in performance as
210 being due to higher noise levels in the measurement (w_m) and/or production (w_p) relative to the identity
211 context. As such, increases in *BIAS* would result in larger w_m , and increases in \sqrt{VAR} , in larger w_p
212 (**Supplementary Figure 2**). Since the early and late inference strategies are associated with increases
213 in *BIAS* and \sqrt{VAR} respectively, we predicted that fitting this model to the data in the remapped context
214 would result in a systematic increase in w_m and not w_p . Model fits supported this prediction: w_m were
215 substantially higher in the remapped context compared to the identity context (**Figure 3B**, also see
216 **Supplementary Table 1**). This result further substantiates the hypothesis that increased SMN in the
217 remapped context led to additional bias consistent with a late Bayesian inference strategy (**Figure 1A**).
218

219 To further validate this conclusion, we formulated a “Late-Inference” model in which we held w_m and w_p
220 constant across contexts and added an additional scalar SMN parameterized by w_t in the remapped
221 context. This model made late inference by virtue of the fact that inference was made after the
222 introduction of w_t . This Late-Inference model accurately captured the tradeoff between bias and
223 variance in both contexts (**Figure 4A**), consistent with our hypothesis that additional bias in the
224 remapped context was driven by increased SMN. We contrasted this model with two alternatives. First,
225 we tested for the necessity of the additional scalar SMN by constructing an “Equal-SMN” model which
226 omitted w_t . This model was unable to simultaneously capture *RMSE*, *BIAS*, and \sqrt{VAR} in both contexts.
227 Importantly, it systematically underestimated the bias in the remapped context (**Figure 4B**), validating
228 the need for additional w_t in the remapped context. The second alternative model contrasted the Late-
229 Inference model with an “Early-Inference” model in which the inference was made prior to the SMN.
230 Similar to the Equal-SMN model, the Early-Inference model failed to capture behavior (**Figure 4B**),
231 highlighting the importance of late inference in explaining subjects’ behavior. The superiority of the Late-
232 Inference model was further supported by a model comparison using a Bayesian information criterion
233 (*BIC*; **Supplementary Table 2**).

234
235 We considered a number of other models, but were unable to create any model that could account for
236 the increased *BIAS* as accurately as the Late-Inference model. Here, we describe two alternative
237 models that predicted some additional bias in the presence of higher SMN but were nonetheless
238 inferior to the Late-Inference model. The first model, which we refer to as “Late-Ignore-SMN”, is a
239 variant of the Late-Inference model in which the observers makes the inference after the addition of

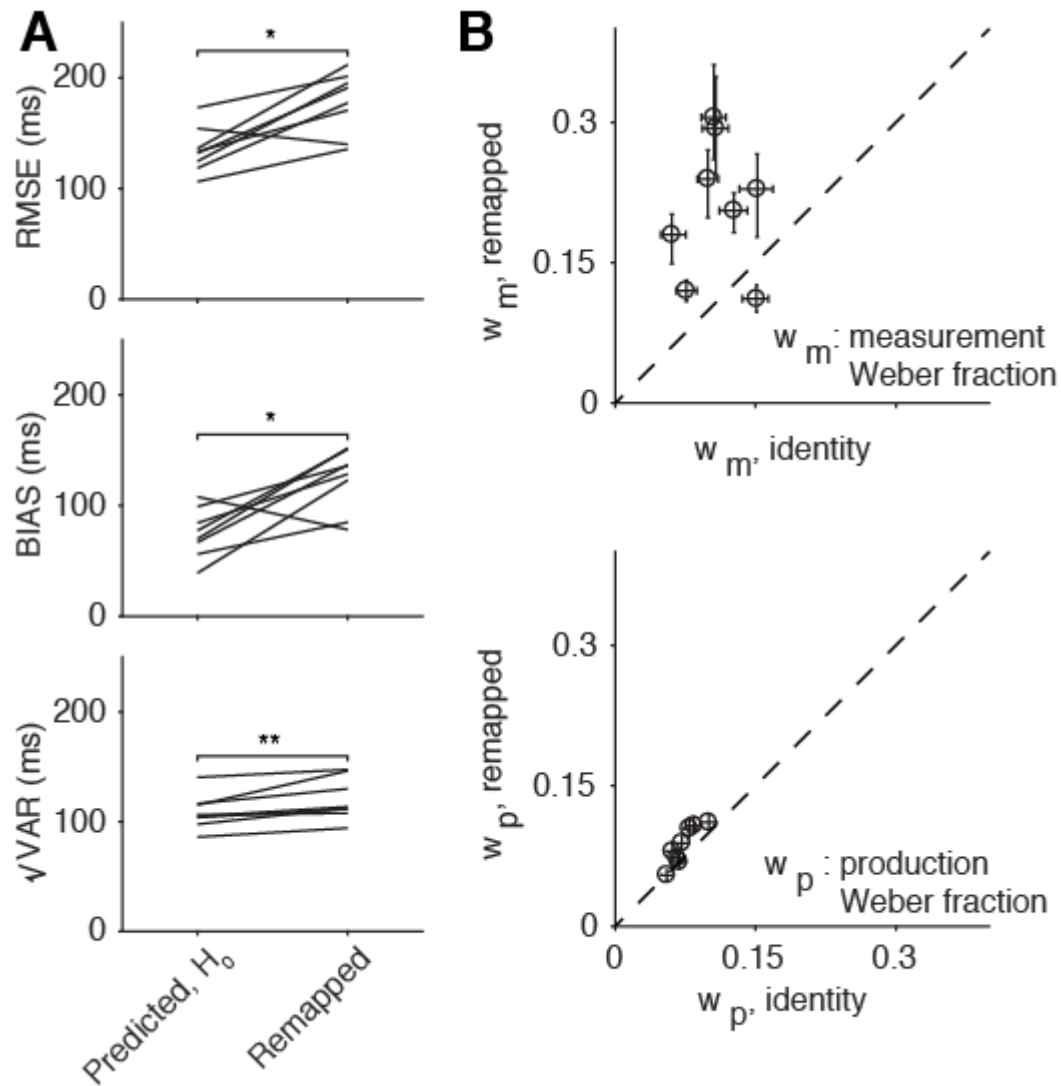
240 SMN (through w_t), but does not take SMN into account. In other words, this is a model of an observer
241 that uses a Late-Inference strategy but does not have an internal model of SMN. The second, which is
242 referred to as the “Observer-Actor” model (Jazayeri and Shadlen 2010; Acerbi, Wolpert, and
243 Vijayakumar 2012), is a variant of the Early-Inference model, which is additionally optimized for scalar
244 variability in the production stages, but not for SMN. Both of these models predicted some degree of
245 increased bias and a substantial (and suboptimal) increase in variability that failed to capture subjects’
246 behavior in the remapped context (**Supplemental Figure 3, Supplementary Table 2**).

247
248 Another explanation that might account for the increased bias in the remapped context is that subjects
249 did not learn the transformation correctly, and instead of applying a gain, simply added a fixed delay to
250 their responses irrespective of the sample interval. Such an offset-adjustment strategy would result in
251 an effective increase in bias and could thus masquerade as a late Bayesian inference strategy. To
252 investigate this possibility, we designed a control experiment with a gain factor of 0.75 instead of 1.5.
253 For a gain of 0.75, a similar offset-adjustment strategy would require subjects to subtract a fixed delay
254 from their responses. This would predict that responses would exhibit less bias than predicted from
255 scaling responses by a factor of 0.75 (i.e., the prediction from the equal SMN hypothesis). However, for
256 the gain of 0.75, similar to the case for a gain of 1.5, subjects’ *RMSE*, *BIAS*, and fits to w_m were higher
257 than predicted by the identity context (**Supplementary Figure 4**). Therefore, the increased bias could
258 not be explained by an offset-adjustment strategy.

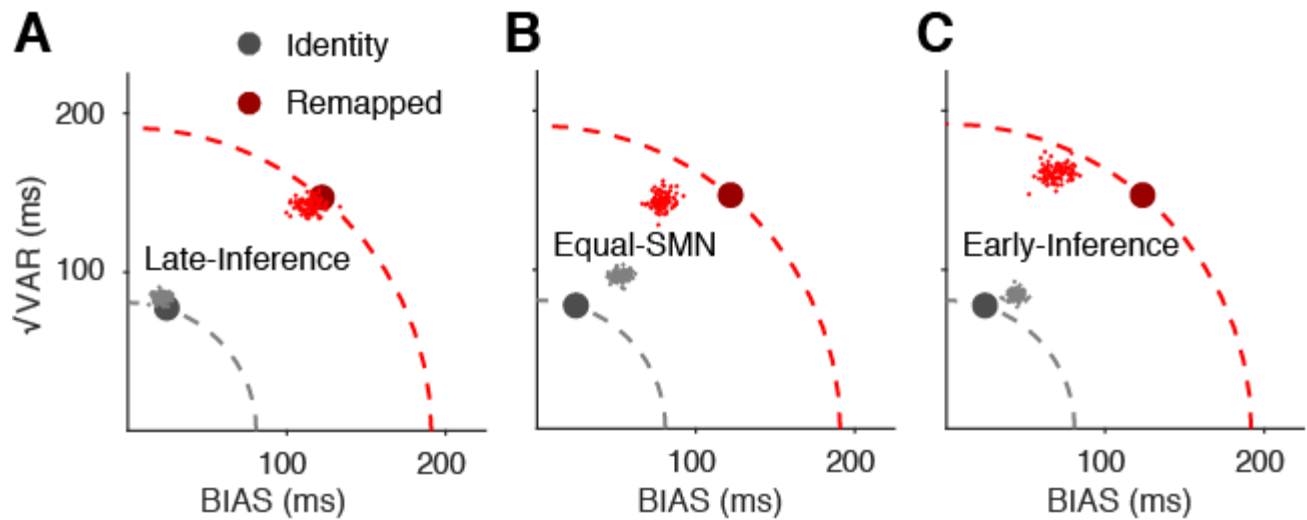


259
 260 **Figure 2.** Time measurement and production task. **A.** Trial structure. Each trial began with the
 261 presentation of a red fixation spot. Subjects had to measure a sample time interval t_s demarcated by
 262 two flashes ("Ready" and "Set") to the left of and above the fixation point, respectively. After Set,
 263 subjects pressed a key ("Go") to produce an interval as close as possible to the correct interval $t_c =$
 264 $gain \times t_s$, where $gain$ changed across two contexts. In the "identity" context, the correct interval was the
 265 same as t_s ($gain = 1$), whereas in the "remapped" context, the gain was 1.5. The position of a stimulus
 266 to the right of the fixation point served as a gain instruction cue. The distance of this stimulus to the
 267 fixation point is equal to or 1.5 times the distance of Ready to the fixation point for the gain of 1 and 1.5,
 268 respectively. After the response, subjects received scaled and signed feedback via the position of a
 269 colored circle (see Methods). **B.** Performance of an example subject in the identity (gray) and
 270 remapped (red) contexts. Filled circles and shaded regions indicate mean response times \pm one
 271 standard deviation; dashed lines represent correct intervals. Solid lines represent the mean responses
 272 of a Bayesian observer model (see Methods) fit to the subject's data separately for the two contexts;
 273 the dash-dot line in the $gain = 1.5$ condition corresponds to the prediction for the remapped context
 274 under the null hypothesis, using parameters of the model fit to the identity context (H_0 : no additional

275 SMN). The subject's behavior shows excess bias beyond what was predicted assuming no additional
276 SMN. **C.** \sqrt{VAR} vs. *BIAS* for the two contexts (gray for identity, and dark red for remapped), as well as
277 the prediction for the remapped context assuming no additional SMN (empty circle). This prediction
278 underestimates *RMSE* indicating larger SMN for the remapped context. The increased *RMSE* was
279 predominantly due to an increase in *BIAS* ("excess bias"). Dashed quarter circles illustrate
280 combinations of *BIAS* vs. \sqrt{VAR} giving rise to equal *RMSE*; error bars are computed from the standard
281 deviation of bootstrapped estimates ($n = 1000$).



282
283 **Figure 3.** Summary of subjects' behavior in the time measurement and production task. (A).
284 Comparison of *RMSE* (top), *BIAS* (middle), and \sqrt{VAR} (bottom) for all subjects. The lines connect
285 values predicted in the remapped context assuming no additional SMN (predicted, H_0 ; left) based on
286 the identity context (i.e. multiplied by the gain of 1.5) to actual values observed from behavior (*gain* =
287 1.5; right). Almost every subject had higher *RMSE* and *BIAS* than was predicted assuming no
288 additional SMN. There was also a small increase in \sqrt{VAR} compared to predictions (*: $p < 0.05$, **: $p <$
289 0.01). (B) Parameters of observer model fits. We fit an observer model (see methods) to each subject's
290 data independently for the two contexts. This model did not explicitly account for SMN, and so any
291 differences in SMN across contexts were reflected in the measurement and production Weber
292 parameters (w_m and w_p). Most subjects were fit with much higher values of w_m (top) in the remapped
293 context, reflecting additional reliance on prior information consistent with a late inference strategy.
294 There was also a more modest increase in w_p for the remapped context (bottom). Error bars represent
295 95% confidence intervals estimated using a bootstrap procedure ($n = 1000$).



296
297 **Figure 4.** Model comparison for the time measurement and production task. (A) Comparison of *BIAS*
298 and \sqrt{VAR} of a typical subject to simulations generated from fits to behavior using the Late-Inference
299 model. The model uses the same measurement and production Weber parameters (w_m and w_p) across
300 the identity (gray) and remapped contexts (red) and introduces additional scalar SMN in the remapped
301 context parameterized by w_t . Large solid circles represent the subject's behavior and small dots
302 represent individual simulations ($n = 100$). (B) Same as A for the Equal-SMN model. This model was
303 identical to the previously described Bayesian observer model (**Supplementary Figure 1; Figure 3**)
304 with w_m and w_p but no w_t . The failure of this model to capture subjects' behavior rejects the null
305 hypothesis that the remapped context can be explained without additional SMN. (C) Same as A for the
306 Early-Inference model. This model includes w_m , w_p , and w_t , but the additional scalar SMN is introduced
307 after the inference stage. The Early-Inference model failed to capture the disparity in *BIAS* between the
308 two contexts when compared with the Late-Inference model, further supporting the late inference
309 hypothesis.

310 **Length measurement and production task**

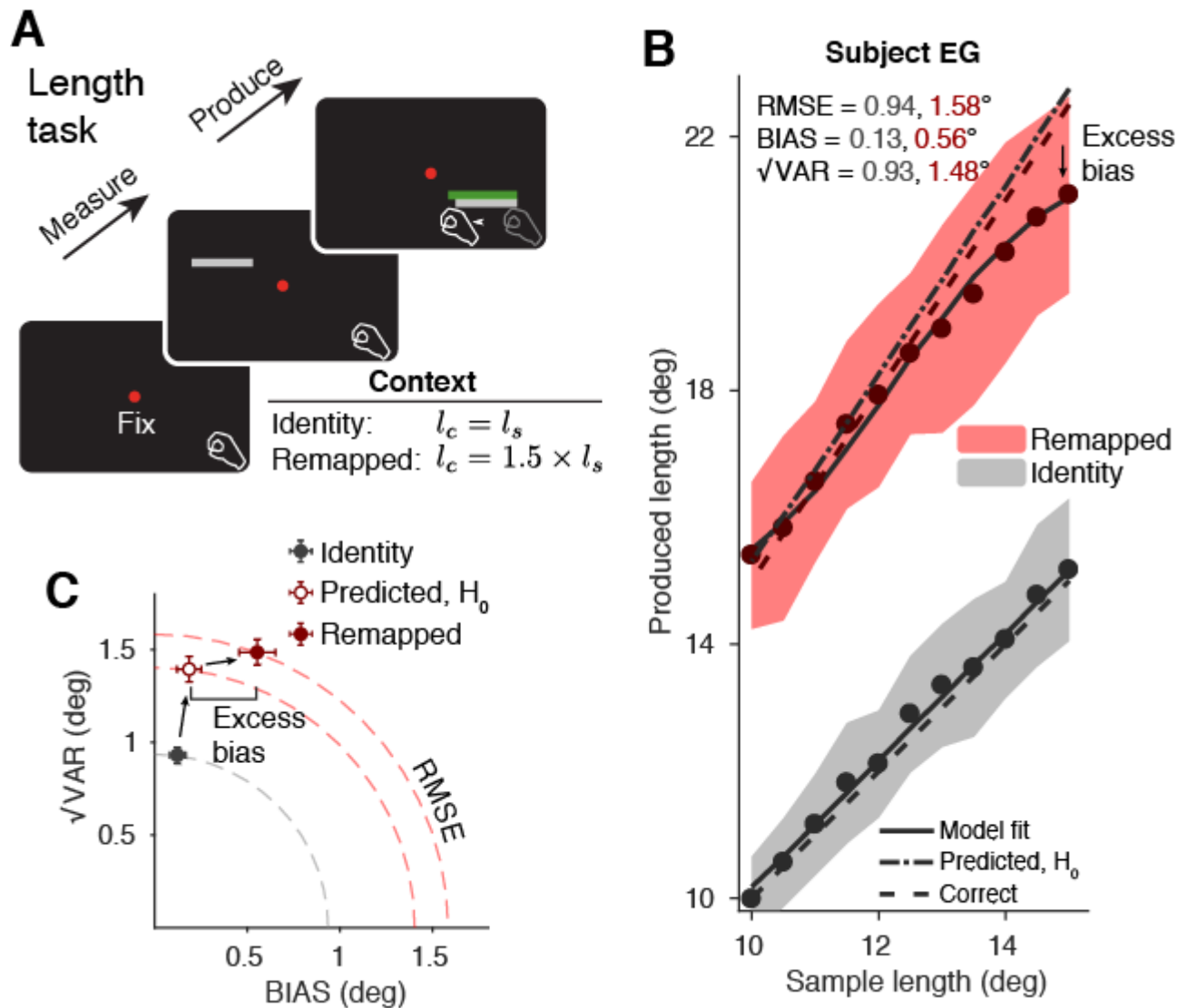
311 In a second experiment, we asked whether SMN degrades performance in a length production task,
312 and whether humans use a late inference strategy to optimize performance in the presence of SMN. To
313 answer this question, we tested the behavior of seven subjects in a task that involved drawing a line
314 whose length was either matched to (identity context) or 1.5 times (remapped context) the length of a
315 visually presented bar (**Figure 5A**). The length of the bar was sampled from a discrete uniform
316 distribution with 11 values ranging between 10 and 15 visual degrees and was presented on a
317 horizontally oriented monitor. After presentation of the visual bar, subjects had to draw a bar by moving
318 a handle that controlled the position of a cursor on the monitor (**Figure 5A**).

319
320 **Figure 5B** shows the behavior of one subject in the length measurement and production task. Similar
321 to the timing task, *RMSE* was higher in the remapped context compared to the identity context
322 suggesting that SMN was larger for the transformation associated with $gain = 1.5$. Moreover, the
323 increase in *RMSE* was associated with an excess bias beyond what was expected from multiplying the
324 observed bias in the identity context by the gain. The higher *RMSE* and *BIAS* was a general finding
325 across subjects (**Figure 6A**) indicating that the length task was also associated with a late Bayesian
326 strategy to compensate for the larger SMN.

327
328 To further validate these results using model comparisons, we first sought to develop an ideal observer
329 model of the length task. In the timing task, the Bayesian observer model we used was based on
330 previous work using a time reproduction task (Jazayeri and Shadlen 2010) and included two
331 parameters: one scaling factor for the measurement noise (w_m), and another for the production noise
332 (w_p). For the length task, we considered the possibility that the production stage might be subject to
333 additional execution noise due to hand movements, as previous work has suggested (Wolpert,
334 Ghahramani, and Jordan 1995; Robert J. van Beers, Haggard, and Wolpert 2004). We compared a
335 model similar to the timing task with scalar measurement and production noise to another model that
336 included an additional signal independent production noise term σ_p . The model with the additional
337 nonscalar production noise provided a better description of behavior despite having an additional
338 parameter (relative BIC of 64, compared to 49 in favor of pure scalar model for the timing task). We
339 therefore proceeded with this scalar-nonscalar model to compare the identity and remapped contexts.

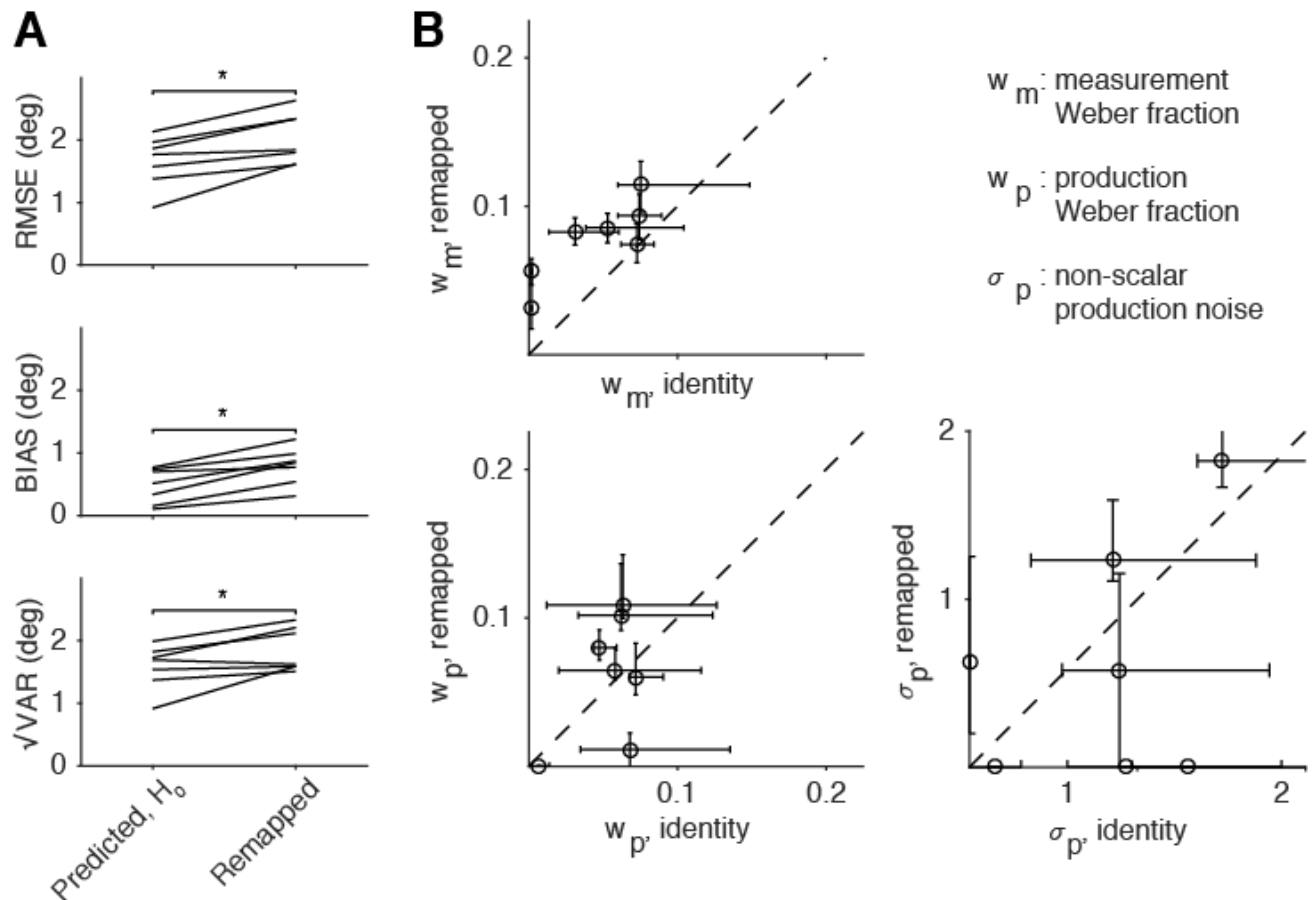
340
341 Similar to the timing task, observer model fits in the remapped context were associated with higher
342 values for w_m and no systematic relationship to w_p and σ_p (**Figure 6B**). These results indicate that the
343 higher SMN in the remapped context is accompanied by higher reliance on prior information, as
344 expected from the late Bayesian inference strategy. This result was further substantiated by a direct
345 model comparison based on BIC showing that the Late-Inference model was best at capturing the data
346 in the remapped context (see **Supplementary Tables 3 & 4** for individual subjects' results and

347 summary).



348
 349 **Figure 5.** Length measurement and production task. **A.** Trial structure. Each trial began with the
 350 presentation of a red fixation spot. Subjects first measured the length l_s of a gray sample bar presented
 351 briefly on an upwards facing monitor. After the sample bar was extinguished, subjects moved a
 352 manipulandum containing a digitizing pen located under the monitor in order to draw a bar which was
 353 as close in length as possible to the correct length $l_c = g \times l_s$. As in the timing task, there were two
 354 contexts: in the identity context, $gain = 1$, whereas in the remapped context, $gain = 1.5$. After the
 355 response, subjects received scaled and signed feedback via the presentation of a gray bar of the
 356 proper length while the subjects' produced bar changed color to red (for an inaccurate response) or
 357 green (for an accurate response; see Methods). **B.** Performance of an example subject in the identity
 358 (gray) and remapped (red) contexts (same format as **Figure 2**). Filled circles and shaded regions
 359 indicate mean response times \pm one standard deviation; dashed lines represent correct intervals. Solid
 360 lines represent the mean responses of a Bayesian observer model (see Methods) fit to the subject's
 361 data separately for the two contexts; the dash-dot line in the $gain = 1.5$ condition corresponds to the
 362 prediction for the remapped context using parameters of the model fit to the identity context (H_0 : no
 363 additional SMN). Comparing the model fit for the remapped context to the no additional SMN prediction,

364 the excess bias towards the mean in the remapped relative to the identity context can be seen. **C.**
365 \sqrt{VAR} vs. *BIAS* for the two contexts (gray for identity, and dark red for remapped), as well as the
366 prediction for the remapped context assuming no additional SMN (empty circle). This prediction
367 underestimates *RMSE* indicating larger SMN for the remapped context. The increased *RMSE* was
368 predominantly due to an increase in *BIAS* (“excess bias”). Dashed quarter circles illustrate
369 combinations of *BIAS* vs. \sqrt{VAR} giving rise to equal *RMSE*; error bars are computed from the standard
370 deviation of bootstrapped estimates ($n = 1000$).



371
 372 **Figure 6.** Summary of subjects' performance in the length production task. **(A)** Comparison of *RMSE*,
 373 *BIAS*, and \sqrt{VAR} for all subjects. The lines connect values predicted in the remapped context based on
 374 simulated data from the observer model fit to individual subjects' behavior for gain of 1 and assuming
 375 no additional SMN (predicted, H_0 ; left) to actual values observed from behavior (*gain* = 1.5; right).
 376 Similar to the timing task, subjects had higher error and were more biased towards the mean than was
 377 predicted assuming no additional SMN in the remapped context. Variability also increased in most
 378 subjects (*: $p < 0.05$). **(B)** Fitting the observer model independently across the two contexts resulted in
 379 higher values of w_m in the remapped context, reflecting additional reliance on prior information
 380 consistent with a late inference strategy. Values for w_p and the non-scalar motor noise parameter σ_p
 381 were not systematically affected by the gain. Error bars represent 95% confidence intervals estimated
 382 using a bootstrap procedure ($n = 1000$).

383 Discussion

384
385 Noise in sensorimotor transformations directly impacts performance. To optimize behavior in the
386 presence of sensorimotor noise, the brain must adopt a late inference strategy that takes sensorimotor
387 noise into account and adjusts motor plans according to the statistics of the outcomes. Our results
388 indicate that subjects compensate for noise in sensorimotor transformations by biasing responses
389 towards the mean of a sensorimotor prior, supporting the hypothesis that humans seek to optimize
390 behavior in the presence of sensorimotor noise by adopting a late inference strategy. This finding
391 extends previous work on Bayesian models of sensory and motor systems, and indicates that the brain
392 circuits are additionally optimized for noise arising from sensorimotor transformations.

393
394 The vast majority of experiments on the application of Bayesian theory to behavior involve some sort of
395 sensorimotor transformation. As we found in our work, and others found in other behavioral settings
396 (Soechting and Flanders 1989b; Gordon, Ghilardi, and Ghez 1994; Pine et al. 1996; McIntyre et al.
397 2000; Sober and Sabes 2005; Churchland, Afshar, and Shenoy 2006; Schlicht and Schrater 2007),
398 sensorimotor transformations are often noisy. Surprisingly however, most Bayesian models do not take
399 SMN into account and formulate Bayesian calculations in terms of sensory inference (Weiss,
400 Simoncelli, and Adelson 2002; Tassinari, Hudson, and Landy 2006; Jazayeri and Shadlen 2010;
401 Ganguli and Simoncelli 2014). This approach may be adequate when the sensory noise is the dominant
402 source of uncertainty (Osborne, Lisberger, and Bialek 2005). However, sensorimotor transformations
403 may generate a substantial fraction of the total noise. Indeed, for the Late-Inference model, which
404 captured behavior most accurately, the transformation noise (w_t) associated with the remapped context
405 was larger than measurement noise (w_m ; **Supplementary Tables 2 & 4**). This suggests that many
406 previous experiments that ignored SMN and yet found the behavior to be optimal might have
407 misattributed SMN to noise in sensory representations (see **Figures 3B & 6B**). This is not surprising as
408 distinguishing between sensory and sensorimotor noise is not straightforward when the two are not
409 independently manipulated. Our experiment was designed to overcome this challenge by comparing
410 identity and remapped sensorimotor contexts and thus manipulating SMN without changing the sensory
411 noise. Finally, it is important to note that our own work is not fully immune to the misattribution of SMN
412 to sensory noise. While we were able to reveal the excess bias due to larger SMN in the remapped
413 context, it is conceivable that SMN was a significant factor in the identity context as well. This might
414 explain why a previous study found time measurement and reproduction task to be more biased than
415 predicted by noise levels in a temporal bisection task (Cicchini et al. 2012). As such, we might have
416 underestimated the importance of SMN by misattributing some portion to SMN to measurement noise
417 in both contexts.

418
419 Our proposal of a late inference strategy unifies various observations in a wide range of sensorimotor

420 tasks. For example, it has been shown that when both visual and proprioceptive information are
421 available, subjects rely more strongly on the modality that had the least transformational complexity
422 (Sober and Sabes 2005). Schlicht and Schrater (Schlicht and Schrater 2007) showed that subjects
423 account for the effects of eye position uncertainty in a grasping task by increasing grip aperture.
424 Another study found that reach movements in 3-dimensional space were consistently biased towards
425 the centroid of target distributions, particularly along the radial (distance) axis, and that this bias was
426 not seen when subjects performed a simpler pointing task which only required wrist movements
427 (Soechting and Flanders 1989b). The authors' interpretation of these results was that the brain
428 implemented linear approximations to the true nonlinear transformations between target location and
429 motor commands (Soechting and Flanders 1989a). However, our results suggest that the bias might be
430 due to a stronger influence of prior information when facing the more challenging sensorimotor task of
431 reaching in 3D. Late inference may also explain response patterns in reaching tasks where biases exist
432 in arm-centered, rather than eye-centered reference frames (Baud-Bovy and Viviani 1998), or in cases
433 where target-dependent bias unexplained by sensory noise is attributed to suboptimal aiming strategies
434 (Tassinari, Hudson, and Landy 2006).

435
436 Moreover, the late inference model provides a natural explanation for why various post-sensory
437 cognitive operations cause additional biases in behavior. Without a late inference strategy, one would
438 expect sources of noise such as memory decay to lead to additional variability. However, a number of
439 experiments have shown that post-sensory noisy computations can lead substantial increases in bias.
440 Examples include mental operations in the presence of memory delays (Moyer et al. 1978; Ashourian
441 and Loewenstein 2011), predictions of complex kinematics (Smith and Vul 2013; Battaglia, Hamrick,
442 and Tenenbaum 2013), and pointing in 3D space under various memory loads (McIntyre et al. 2000). In
443 all these cases, the additional biases can be straightforwardly accounted for by considering the
444 possibility that the brain has an internal model of post-sensory noisy transformations and compensates
445 for them by using its prior knowledge about the desired outcomes.

446
447 Late inference may seem at odds with recent proposals that priors based of natural stimuli may already
448 be applied at low-level sensory areas (Weiss, Simoncelli, and Adelson 2002; Girshick, Landy, and
449 Simoncelli 2011). However, the late inference model is fully compatible with early integration of sensory
450 inputs with priors as well as multiple stage of updating the posterior (Ma et al. 2006; Beck et al. 2008;
451 Ganguli and Simoncelli 2014; Ma and Jazayeri 2014). The key constraint imposed by the late inference
452 strategy is simply for the brain to delay extracting a point estimate from the posterior distribution to as
453 late as possible (Simoncelli 2009).

454
455 Finally, our results bear on the computational principles that govern brain function when information
456 undergoes multiple processing stages. We found that the brain computations are optimized for

457 sensorimotor transformations suggesting that the inference is made after the addition of sensorimotor
458 noise. However, late inference is not a special requirement that only applies to sensorimotor noise. The
459 passage of information in the simplest visuomotor task from the primary visual cortex to downstream
460 visual areas to sensorimotor cortex to movement control circuits undergoes many stages of processing.
461 Each stage of processing is likely to have its own private noise and can thus add to the overall
462 variability. Regardless of the task and where the noise is added, the optimal strategy is to delay
463 inference until after the final stages of processing (Simoncelli 2009). This applies even when
464 intermediate transformations are trivial, as must be the case when most of the error can be attributed to
465 sensory processing (Osborne, Lisberger, and Bialek 2005). This optimality consideration coupled with
466 evidence from our work that the brain does indeed delay inferences until after the introduction of
467 sensorimotor noise suggest that brain circuits may employ Bayesian inference as an inherent
468 computational principle.

469 **Methods**

470

471 **Subjects**

472 Human subjects aged 18-65 years participated in this study after giving informed consent. All
473 experiments were approved by the Committee on the Use of Humans as Experimental Subjects at the
474 Massachusetts Institute of Technology. The study consisted of two experiments: a time interval
475 estimation and production task (Experiment 1), and a length estimation and production task
476 (Experiment 2). A group of 9 subjects participated in Experiment 1 (8 for gain = 1.5 and 9 for gain =
477 0.75), and a mostly different group of 7 subjects participated in Experiment 2 (1 subject participated in
478 both experiments). All subjects had normal or corrected-to-normal vision.

479

480 **Procedures**

481 Experimental sessions lasted approximately 45-60 minutes. Each subject completed 1-2 sessions per
482 week. Experiments were controlled by an open-source software (MWorks; <http://mworks-project.org/>).
483 All stimuli were presented on a black background. Although eye movements were not monitored, all
484 trials began with central fixation spot that subjects were asked to hold their gaze on throughout the trial.
485 In Experiment 1, subjects viewed all stimuli binocularly from a distance of approximately 67 cm on
486 either a 23-inch Apple A1082 LCD monitor at a resolution of 1900 x 1200 driven by an Intel Macintosh
487 Mac Pro computer, or a 24-inch early 2009 Apple Mac Pro at a refresh rate of 60 Hz in a dark, quiet
488 room. In this experiment, responses were registered on a standard Apple Keyboard connected to the
489 experimental machine. In Experiment 2, subjects viewed stimuli from above on a 21.5-inch Samsung
490 SyncMaster SA200 monitor, and responses were registered using a pen digitizer tablet (Wacom
491 Intuos5 touch); the stylus was fixed at a vertical position inside a custom printed handle which subjects
492 grasped.

493

494 **Behavioral tasks**

495 Our objective in both experiments was to investigate the effect of sensorimotor noise (SMN) on
496 performance. To do so, each experiment consisted of two sensorimotor contexts, an “identity” context,
497 and a more challenging “remapped” context that was expected to involve higher levels of SMN. In each
498 experiment, human subjects measured a scalar sensory quantity (time interval in Experiment 1, and
499 length in Experiment 2) drawn from a prior distribution. In the “identity” context, subjects had to
500 reproduce the sensory quantity (the sample), and in the “remapped” context, they had to produce the
501 same quantity multiplied by a gain factor. Subjects whose responses for the shortest and longest stimuli
502 in the identity context were at least one d' (d -prime) apart were invited to participate in the main
503 experiment.

504

505 **Experiment 1: Time interval estimation and production task.** The behavioral task used in

506 Experiment 1 was a variant of the Ready, Set, Go task used in a previous study (Jazayeri and Shadlen
507 2010). Subjects had to measure a sample interval drawn from an 11-point discrete uniform distribution
508 between 600 and 1000 ms, then immediately produce an interval that was equal to the sample interval
509 multiplied by a gain factor. The sample interval was demarcated by two visual flashes (“Ready” and
510 “Set”) located to the left and above a fixation point at the center of a computer monitor. The production
511 interval was defined as the interval between the onset of the second flash and the response (key press)
512 of the subject. In the identity context, the gain was 1, whereas in the remapped contexts the gain was
513 either 1.5 or 0.75. The gain was fixed in each behavioral session and was communicated at the
514 beginning of each session as either “same,” “shorter,” or “longer.” The gain was also evident on every
515 trials: the ratio of the horizontal distance between the Ready flash to the left of the fixation point and a
516 “Go” cue to the right fixation was set by the gain factor. Following each response, subjects were given
517 feedback regarding their response via a round marker displayed a distance from the Go cue
518 proportional to the error and regarding the trial outcome via the color of the marker. A green marker
519 indicated a “hit” and a white marker indicated a “miss.” Subjects completed two consecutive sessions of
520 600 trials for each gain; the hit/miss threshold was on a staircase for the first session and fixed for the
521 second session at the mean of the last 100 trials of the first session. Analyses were performed using
522 data from the second sessions. All subjects completed the “identity” context sessions first, followed by
523 either the gain of 1.5 or gain of 0.75, selected pseudorandomly for each subject.

524
525 **Experiment 2: Length estimation and production task.** The behavioral task used in Experiment 2
526 was conceptually similar to the first in that subjects produced a scalar quantity multiplied by a gain
527 factor. However, instead of a time interval, subjects measured and produced visually presented lines
528 drawn from an 11-point discrete uniform distribution between 10 and 15 degrees visual angle. To
529 produce the length, subjects had to move a manipulandum underneath a horizontally positioned
530 computer monitor. In each trial, after subjects positioned the manipulandum at the perimeter of the
531 screen, a horizontal line flashed for 500 ms, after which subjects had 1200 ms to move the
532 manipulandum inward to the final response position. Two small vertical bars, one positioned at the
533 initial location of the manipulandum and one tracking the horizontal location of the bar, provided online
534 visual feedback during the response. The produced length was measured as the distance between the
535 two vertical bars at the end of the response period. The gain in the identity and remapped contexts was
536 1 and 1.5, respectively. The gain was communicated by telling subjects to produce either “the same as”
537 or “one and a half times” the length of the sample. Response feedback was similar to the interval
538 production task: following each response, the produced length was shown as a line between the marker
539 bars (green for hit and red for miss), and the correct length was displayed immediately beneath in gray.
540 Subjects completed four sessions total with each session comprising two blocks of 150 trials of identity
541 and remapped trials for a total of 600 trials per session. The error threshold for each gain was on a one-
542 up one-down staircase for the first two sessions and fixed for the final two sessions at the mean of the

543 last 100 trials for each gain. The order of blocks associated with the identity and remapped blocks was
544 pseudorandomized across subjects.

545 **Data analysis**

546 Behavioral performance in all tasks was quantified with three statistics (Jazayeri and Shadlen 2010):
547 *BIAS*, \sqrt{VAR} , and *RMSE*. *BIAS* summarizes the difference between average and correct responses and is
548 defined as

$$549 \quad BIAS = \sqrt{\sum_{i=1}^N bias_i^2} \quad (1)$$

551 where *bias* is the difference between the mean response and correct response for a given sample
552 interval. \sqrt{VAR} summarizes the variability of responses:

$$553 \quad \sqrt{VAR} = \sqrt{\sum_{i=1}^N var_i} \quad (2)$$

554 where *var* is the variance of the responses for a particular sample interval. Because samples were
555 drawn randomly, it was not the case that the number of trials for each sample was exactly the same.
556 Therefore, averages of for *BIAS* and \sqrt{VAR} were normalized across samples according to the number
557 of trials presented. Finally, *RMSE* was calculated as:

$$558 \quad RMSE = \sqrt{(\sqrt{VAR})^2 + BIAS^2} \quad (3)$$

559 The three quantities are related through a sum of squares: $RMSE^2 = (\sqrt{VAR})^2 + BIAS^2$ (see **Figure 1B**).
560 Prior to analyzing data, we identified and removed “lapse” trials for each subject. This involved finding
561 and removing trials for which responses were greater than three standard deviations from the mean
562 response for a particular sample quantity and context, and which was performed twice iteratively.

564 **Model descriptions and fitting procedure**

565 We employed a Bayesian model previously shown to capture the behavior of human subjects in the
566 timing task (Jazayeri and Shadlen 2010). The model consists of three stages: a noisy measurement
567 stage, a deterministic Bayesian inference stage, and a noisy production stage (**Supplementary Figure**
568 **1**). The noisy measurement t_m (t = time) is generated according to the noise model $p(t_m|t_s)$, then used
569 to generate an inference t_i which minimizes the expected squared error between t_i and t_s given t_m :

$$571 \quad t_i = f(t_m) = \underset{t}{\operatorname{argmin}} \int_{t_s} (t - t_s)^2 p(t_s|t_m) \pi(t_s) dt_s = E[t_s|t_m] \quad (4)$$

572

573 Where $\pi(t_s)$ represents the observer's "prior" belief about t_s . The inference, which can be thought of as
574 a perceptual estimate, is the expected value of the sample interval given the measurement. The model
575 then generates t_p according to the production noise model $p(t_p|t_i)$. $p(t_m|t_s)$ and $p(t_p|t_i)$ were formulated
576 as Gaussian distributions with means t_s and t_i , respectively, and standard deviations that scaled with
577 the respective means. This model has two free parameters, w_m and w_p , which represent the Weber
578 fractions (i.e., ratio of standard deviation to mean) for $p(t_m|t_s)$ and $p(t_p|t_i)$, respectively. Generally, the
579 model captures high response variability by increases in w_p , and large response biases towards the
580 mean of the prior by increases in w_m . As a corollary, increases in w_p have a comparably larger effect
581 on total error (**Supplementary Figure 2**).

582
583 This model was used in three ways. First, we used it to predict responses in the remapped context from
584 fits of the model to the identity context (without changing the model parameters). We used this
585 approach to generate predictions for the null hypothesis that the remapped context did not engender
586 additional SMN. Second, we fit this model to the behavior but allowed w_m and w_p to take on different
587 values in the two contexts. We used this approach to distinguish between the early and late inference
588 hypotheses. Based on the behavior of this model (**Supplementary Figure 2**) we expected a late
589 inference strategy would cause an increase in response biases and lead to systematic increases in the
590 fit to w_m but not w_p . Third, we used the model to fit the data combined across the two contexts. This
591 approach would succeed under the null hypothesis that the two contexts have the same level of SMN.
592 We refer to this model the "Equal-SMN" model.

593
594 We also developed an "Early-Inference" and a "Late-Inference" model, which included an additional
595 parameter, w_t , to capture putative additional SMN in the remapped context. These models were fitted to
596 the combined data in the two contexts. In the Early-Inference model, Bayesian inference was applied to
597 the sensory measurement stage, and SMN was added to the production stage (after inference). To do
598 so, we formulated the production stage such that $p(t_p|t_i)$ was a scalar Gaussian distribution with mean
599 of $gain \times t_i$ and modified Weber fraction $\sqrt{(w_p^2 + w_t^2)}$. In contrast, for the Late-Inference model, the effect
600 of SMN was applied prior to the inference stage by drawing samples of the "remapped" measurement
601 from a Gaussian distribution $p(t_i|t_s)$ with mean of $gain \times t_s$ and Weber fraction $\sqrt{(w_m^2 + w_t^2)}$, where t_t
602 (transformed interval) represents t_m multiplied by the remapping gain.

603
604 In the Early-Inference model, the prior distribution corresponded to the sensory variable (i.e., prior to
605 transformation), whereas in the Late-Inference mode it was formulated based on the transformed
606 sensory variable (i.e., sensory variable multiplied by the gain). This modified prior represents the
607 observer's belief about the correct interval and can be viewed as a sensorimotor rather than sensory
608 prior.

609

610 Model parameters were fit by maximizing the log-likelihood of subjects' responses given the sample
611 values and gain. The maximization was done using the fminsearch command in MATLAB (Mathworks).
612 Model fitting and simulation involved numerical integration over the posterior distribution using
613 Simpson's rule. Parameter searches were repeated ten times each with different parameter
614 initialization, and results were inspected for consistency.

BIAS	Summary bias
l_c	correct length interval
l_s	sample length interval
RMSE	Root mean square error
σ_p	Production standard deviation
SMN	Sensorimotor noise
t_c	Correct time interval
t_i	Inferred time interval
t_m	Measured time interval
t_p	Produced time interval
t_s	Sample time interval
$\sqrt{\text{VAR}}$	Summary standard deviation
w_m	Measurement Weber fraction
w_p	Production Weber fraction
w_t	Sensorimotor transformation Weber fraction
deg	Visual degrees
ms	Milliseconds
H_0	Null hypothesis

615

616 **Table 1.** Variables and abbreviations.

617 References

- 618 Acerbi, Luigi, Daniel M. Wolpert, and Sethu Vijayakumar. 2012. "Internal Representations of Temporal
619 Statistics and Feedback Calibrate Motor-Sensory Interval Timing." *PLoS Computational Biology* 8
620 (11): e1002771. doi:10.1371/journal.pcbi.1002771.
- 621 Alais, David, and David Burr. 2004. "The Ventriloquist Effect Results from near-Optimal Bimodal
622 Integration." *Current Biology: CB* 14 (3). Elsevier: 257–62. doi:10.1016/j.cub.2004.01.029.
- 623 Ashourian, Paymon, and Yonatan Loewenstein. 2011. "Bayesian Inference Underlies the Contraction
624 Bias in Delayed Comparison Tasks." *PloS One* 6 (5): e19551. doi:10.1371/journal.pone.0019551.
- 625 Battaglia, Peter W., Jessica B. Hamrick, and Joshua B. Tenenbaum. 2013. "Simulation as an Engine of
626 Physical Scene Understanding." *Proceedings of the National Academy of Sciences of the United
627 States of America* 110 (45): 18327–32. doi:10.1073/pnas.1306572110.
- 628 Battaglia, Peter W., Robert A. Jacobs, and Richard N. Aslin. 2003. "Bayesian Integration of Visual and
629 Auditory Signals for Spatial Localization." *Journal of the Optical Society of America. A, Optics,
630 Image Science, and Vision* 20 (7). osapublishing.org: 1391–97.
631 <http://www.ncbi.nlm.nih.gov/pubmed/12868643>.
- 632 Baud-Bovy, G., and P. Viviani. 1998. "Pointing to Kinesthetic Targets in Space." *The Journal of
633 Neuroscience: The Official Journal of the Society for Neuroscience* 18 (4). Soc Neuroscience:
634 1528–45. <https://www.ncbi.nlm.nih.gov/pubmed/9454859>.
- 635 Beck, Jeffrey M., Wei Ji Ma, Roozbeh Kiani, Tim Hanks, Anne K. Churchland, Jamie Roitman, Michael
636 N. Shadlen, Peter E. Latham, and Alexandre Pouget. 2008. "Probabilistic Population Codes for
637 Bayesian Decision Making." *Neuron* 60 (6): 1142–52. doi:10.1016/j.neuron.2008.09.021.
- 638 Beers, R. J. van, A. C. Sittig, and J. J. Gon. 1999. "Integration of Proprioceptive and Visual Position-
639 Information: An Experimentally Supported Model." *Journal of Neurophysiology* 81 (3). Am
640 Physiological Soc: 1355–64. <https://www.ncbi.nlm.nih.gov/pubmed/10085361>.
- 641 Beers, Robert J. van, Patrick Haggard, and Daniel M. Wolpert. 2004. "The Role of Execution Noise in
642 Movement Variability." *Journal of Neurophysiology* 91 (2): 1050–63. doi:10.1152/jn.00652.2003.
- 643 Bresciani, Jean-Pierre, Franziska Dammeier, and Marc O. Ernst. 2008. "Tri-Modal Integration of Visual,
644 Tactile and Auditory Signals for the Perception of Sequences of Events." *Brain Research Bulletin*
645 75 (6). Elsevier: 753–60. doi:10.1016/j.brainresbull.2008.01.009.
- 646 Burge, Johannes, Marc O. Ernst, and Martin S. Banks. 2008. "The Statistical Determinants of
647 Adaptation Rate in Human Reaching." *Journal of Vision* 8 (4). jov.arvojournals.org: 20.1–19.
648 doi:10.1167/8.4.20.
- 649 Butler, John S., Stuart T. Smith, Jennifer L. Campos, and Heinrich H. Bühlhoff. 2010. "Bayesian
650 Integration of Visual and Vestibular Signals for Heading." *Journal of Vision* 10 (11).
651 jov.arvojournals.org: 23. doi:10.1167/10.11.23.
- 652 Churchland, Mark M., Afsheen Afshar, and Krishna V. Shenoy. 2006. "A Central Source of Movement
653 Variability." *Neuron* 52 (6): 1085–96. doi:10.1016/j.neuron.2006.10.034.

- 654 Cicchini, Guido Marco, Roberto Arrighi, Luca Cecchetti, Marco Giusti, and David C. Burr. 2012.
655 “Optimal Encoding of Interval Timing in Expert Percussionists.” *The Journal of Neuroscience: The*
656 *Official Journal of the Society for Neuroscience* 32 (3): 1056–60. doi:10.1523/JNEUROSCI.3411-
657 11.2012.
- 658 Ernst, Marc O., and Martin S. Banks. 2002. “Humans Integrate Visual and Haptic Information in a
659 Statistically Optimal Fashion.” *Nature* 415 (6870): 429–33. doi:10.1038/415429a.
- 660 Gallistel, C. R., and J. Gibbon. 2000. “Time, Rate, and Conditioning.” *Psychological Review* 107 (2).
661 psycnet.apa.org: 289–344. <https://www.ncbi.nlm.nih.gov/pubmed/10789198>.
- 662 Ganguli, Deep, and Eero P. Simoncelli. 2014. “Efficient Sensory Encoding and Bayesian Inference with
663 Heterogeneous Neural Populations.” *Neural Computation* 26 (10). MIT Press: 2103–34.
664 doi:10.1162/NECO_a_00638.
- 665 Girshick, Ahna R., Michael S. Landy, and Eero P. Simoncelli. 2011. “Cardinal Rules: Visual Orientation
666 Perception Reflects Knowledge of Environmental Statistics.” *Nature Neuroscience* 14 (7): 926–32.
667 doi:10.1038/nn.2831.
- 668 Gordon, James, Maria Felice Ghilardi, and Claude Ghez. 1994. “Accuracy of Planar Reaching
669 Movements.” *Experimental Brain Research. Experimentelle Hirnforschung. Experimentation*
670 *Cerebrale* 99 (1). Springer-Verlag: 97–111. doi:10.1007/BF00241415.
- 671 Jazayeri, Mehrdad, and Michael N. Shadlen. 2010. “Temporal Context Calibrates Interval Timing.”
672 *Nature Neuroscience* 13 (8). Nature Publishing Group: 1020–26. doi:10.1038/nn.2590.
- 673 Kersten, Daniel, Pascal Mamassian, and Alan Yuille. 2004. “Object Perception as Bayesian Inference.”
674 *Annual Review of Psychology* 55: 271–304. doi:10.1146/annurev.psych.55.090902.142005.
- 675 Körding, Konrad P., Shih-Pi Ku, and Daniel M. Wolpert. 2004. “Bayesian Integration in Force
676 Estimation.” *Journal of Neurophysiology* 92 (5). Am Physiological Soc: 3161–65.
677 doi:10.1152/jn.00275.2004.
- 678 Körding, Konrad P., and Daniel M. Wolpert. 2004. “Bayesian Integration in Sensorimotor Learning.”
679 *Nature* 427 (6971): 244–47. doi:10.1038/nature02169.
- 680 Landy, Michael S., Julia Trommershäuser, and Nathaniel D. Daw. 2012. “Dynamic Estimation of Task-
681 Relevant Variance in Movement under Risk.” *The Journal of Neuroscience: The Official Journal of*
682 *the Society for Neuroscience* 32 (37): 12702–11. doi:10.1523/JNEUROSCI.6160-11.2012.
- 683 Ma, Wei Ji, Jeffrey M. Beck, Peter E. Latham, and Alexandre Pouget. 2006. “Bayesian Inference with
684 Probabilistic Population Codes.” *Nature Neuroscience* 9 (11): 1432–38. doi:10.1038/nn1790.
- 685 Ma, Wei Ji, and Mehrdad Jazayeri. 2014. “Neural Coding of Uncertainty and Probability.” *Annual*
686 *Review of Neuroscience* 37. annualreviews.org: 205–20. doi:10.1146/annurev-neuro-071013-
687 014017.
- 688 McIntyre, J., F. Stratta, J. Droulez, and F. Lacquaniti. 2000. “Analysis of Pointing Errors Reveals
689 Properties of Data Representations and Coordinate Transformations Within the Central Nervous
690 System.” *Neural Computation* 12 (12): 2823–55. doi:10.1162/089976600300014746.

- 691 Moyer, R. S., D. R. Bradley, M. H. Sorensen, C. Whiting, and D. P. Mansfield. 1978. "Psychophysical
692 Functions for Perceived and Remembered Size." *Science* 200 (4339): 330–32.
693 doi:10.1126/science.635592.
- 694 Osborne, Leslie C., Stephen G. Lisberger, and William Bialek. 2005. "A Sensory Source for Motor
695 Variation." *Nature* 437 (7057): 412–16. doi:10.1038/nature03961.
- 696 Pine, Z. M., J. W. Krakauer, J. Gordon, and C. Ghez. 1996. "Learning of Scaling Factors and Reference
697 Axes for Reaching Movements." *Neuroreport* 7 (14). journals.lww.com: 2357–61.
698 <https://www.ncbi.nlm.nih.gov/pubmed/8951852>.
- 699 Rakitin, B. C., J. Gibbon, T. B. Penney, C. Malapani, S. C. Hinton, and W. H. Meck. 1998. "Scalar
700 Expectancy Theory and Peak-Interval Timing in Humans." *Journal of Experimental Psychology.*
701 *Animal Behavior Processes* 24 (1): 15–33. <http://www.ncbi.nlm.nih.gov/pubmed/9438963>.
- 702 Schlicht, Erik J., and Paul R. Schrater. 2007. "Impact of Coordinate Transformation Uncertainty on
703 Human Sensorimotor Control." *Journal of Neurophysiology* 97 (6): 4203–14.
704 doi:10.1152/jn.00160.2007.
- 705 Simoncelli, Eero P. 2009. "Optimal Estimation in Sensory Systems." *The Cognitive Neurosciences, IV.*
706 MIT Press, 525–35. <http://www.cns.nyu.edu/~rinzel/CMNSS10/simoncelli09a.pdf>.
- 707 Smith, Kevin A., and Edward Vul. 2013. "Sources of Uncertainty in Intuitive Physics." *Topics in*
708 *Cognitive Science* 5 (1): 185–99. doi:10.1111/tops.12009.
- 709 Sober, Samuel J., and Philip N. Sabes. 2005. "Flexible Strategies for Sensory Integration during Motor
710 Planning." *Nature Neuroscience* 8 (4): 490–97. doi:10.1038/nn1427.
- 711 Soechting, J. F., and M. Flanders. 1989a. "Errors in Pointing Are due to Approximations in
712 Sensorimotor Transformations." *Journal of Neurophysiology* 62 (2). Am Physiological Soc: 595–
713 608. <http://www.ncbi.nlm.nih.gov/pubmed/2769350>.
- 714 Soechting, J. F., and M. Flanders. 1989b. "Sensorimotor Representations for Pointing to Targets in
715 Three-Dimensional Space." *Journal of Neurophysiology* 62 (2): 582–94.
716 <http://www.ncbi.nlm.nih.gov/pubmed/2769349>.
- 717 Tassinari, Hadley, Todd E. Hudson, and Michael S. Landy. 2006. "Combining Priors and Noisy Visual
718 Cues in a Rapid Pointing Task." *The Journal of Neuroscience: The Official Journal of the Society*
719 *for Neuroscience* 26 (40): 10154–63. doi:10.1523/JNEUROSCI.2779-06.2006.
- 720 Trommershäuser, Julia, Sergei Gepshtein, Laurence T. Maloney, Michael S. Landy, and Martin S.
721 Banks. 2005. "Optimal Compensation for Changes in Task-Relevant Movement Variability." *The*
722 *Journal of Neuroscience: The Official Journal of the Society for Neuroscience* 25 (31): 7169–78.
723 doi:10.1523/JNEUROSCI.1906-05.2005.
- 724 Weiss, Yair, Eero P. Simoncelli, and Edward H. Adelson. 2002. "Motion Illusions as Optimal Percepts."
725 *Nature Neuroscience* 5 (6). Nature Publishing Group: 598–604. doi:10.1038/nn0602-858.
- 726 Wolpert, D. M., Z. Ghahramani, and M. I. Jordan. 1995. "An Internal Model for Sensorimotor
727 Integration." *Science* 269 (5232): 1880–82. <https://www.ncbi.nlm.nih.gov/pubmed/7569931>.

728 Wolpert, D. M., Z. Ghahramani, and M. I. Jordan. 1995. "An Internal Model for Sensorimotor
729 Integration." *Science* 269 (5232): 1880–82. <https://www.ncbi.nlm.nih.gov/pubmed/7569931>.

730 **Manuscript Supplement**

731

732 **Additional models**

733 We considered two additional models: the Late-Ignore-SMN model and the Observer-Actor model, both
734 of which predicted more bias than the Early-Inference and Equal-SMN models. However both models
735 also predicted a substantial increase in variance (**Supplemental Figure 3**), which deviated from
736 subjects' behavior.

737

738 **The Late-Ignore-SMN model**

739 This model utilizes a late inference stage, but the additional noise from sensorimotor transformations is
740 ignored. More concretely, the model assumes that variability prior to inference is determined by an
741 effective Weber fraction of $\sqrt{(w_m^2 + w_t^2)}$ but that subjects compute the posterior based on the incorrect
742 assumption that the Weber fraction was w_m . In other words, the inference function $f()$ ignores w_t . The
743 reason why ignored SMN causes an increase in bias in the Late-Ignore model may be somewhat
744 counterintuitive. To understand this, let us examine the computations that underlie Bayesian inference
745 in the presence and absence of SMN. In the absence of SMN, there would be a one-to-one
746 correspondence between a measurement and its transformation. For measurements (and
747 transformations thereof) that are farther away from the mean of the uniform prior, the nonlinear
748 inference function (**Supplementary Figure 1, middle panel**) causes more bias in the inferred values.
749 However, the magnitude of this bias would be the same for both early and late inference because of the
750 one-to-one correspondence between a measurement and its transformation. This situation changes
751 however in the presence of SMN. SMN makes the result of this transformation stochastic such that a
752 single measured interval leads to a distribution of transformed measurements. Therefore, the
753 magnitude of bias associated with a measurement has to be computed as an expectation across the
754 distribution of transformed measurements. Since the inference function is nonlinear, it
755 disproportionately biases transformed measurements that are farther away from the mean of the prior
756 distribution (and in particular, outside the support of the uniform prior) leading to an overall increase in
757 the magnitude of the bias.

758

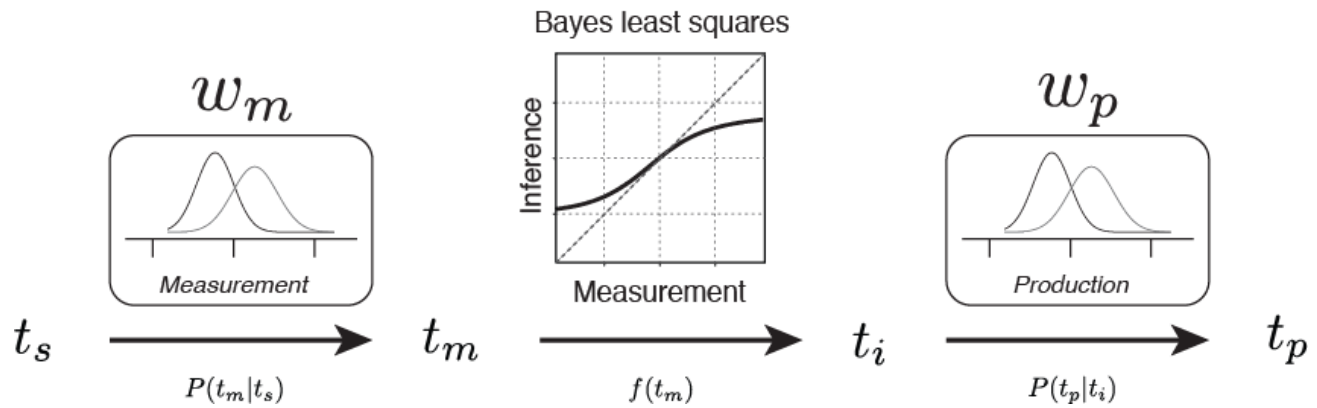
759 While the Late-Ignore-SMN model was able to accommodate more bias, it was not enough to capture
760 the excess bias observed in the data. The model also predicted substantially increased variance, as
761 well as a skewing of response distributions away from the correct response (see **Supplementary**
762 **Figure 3**). We also examined the behavior of the Late-Ignore-SMN model under the assumption that
763 observers approximate uniform priors as Gaussian-like functions as was suggested previously (Acerbi,
764 Wolpert, and Vijayakumar 2012; Cicchini et al. 2012). This possibility reduces the amount of bias
765 introduced by the Late-Ignore-SMN model (data not shown), and further diminishes its utility as a viable
766 model for the observed biases in subjects' behavior.

767 **The Observer-Actor model**

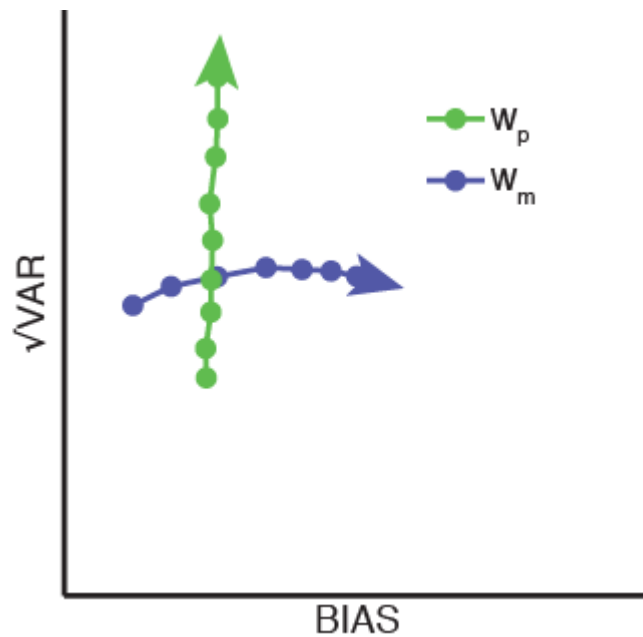
768 This is a variant of the Early-Inference model for which inference is made after the sensory
769 measurement stage and the production stage is modeled by a Gaussian with mean of $gain \times t_i$ and
770 Weber Fraction $\sqrt{(w_p^2 + w_t^2)}$. However, following previous work showing that humans account for
771 response variability when planning actions (Trommershäuser et al. 2005; Landy, Trommershäuser, and
772 Daw 2012) we augmented the inference stage so that the early inference would take into account the
773 scalar post-inference variability due to the transformation and production (Acerbi, Wolpert, and
774 Vijayakumar 2012). The optimal inference under the Observer-Actor model can be computed by
775 marginalizing over the distribution of produced values, $p(t_p|t_i)$:

$$776 \quad t_i = f(t_m) = \underset{t}{\operatorname{argmin}} \int_{t_s} \int_{t_p} (t - t_s)^2 p(t_s | t_m) p(t_p | t) \pi(t_s) dt_p dt_m = \frac{E[t_s | t_m]}{1 + \sqrt{w_p^2 + w_t^2}}$$

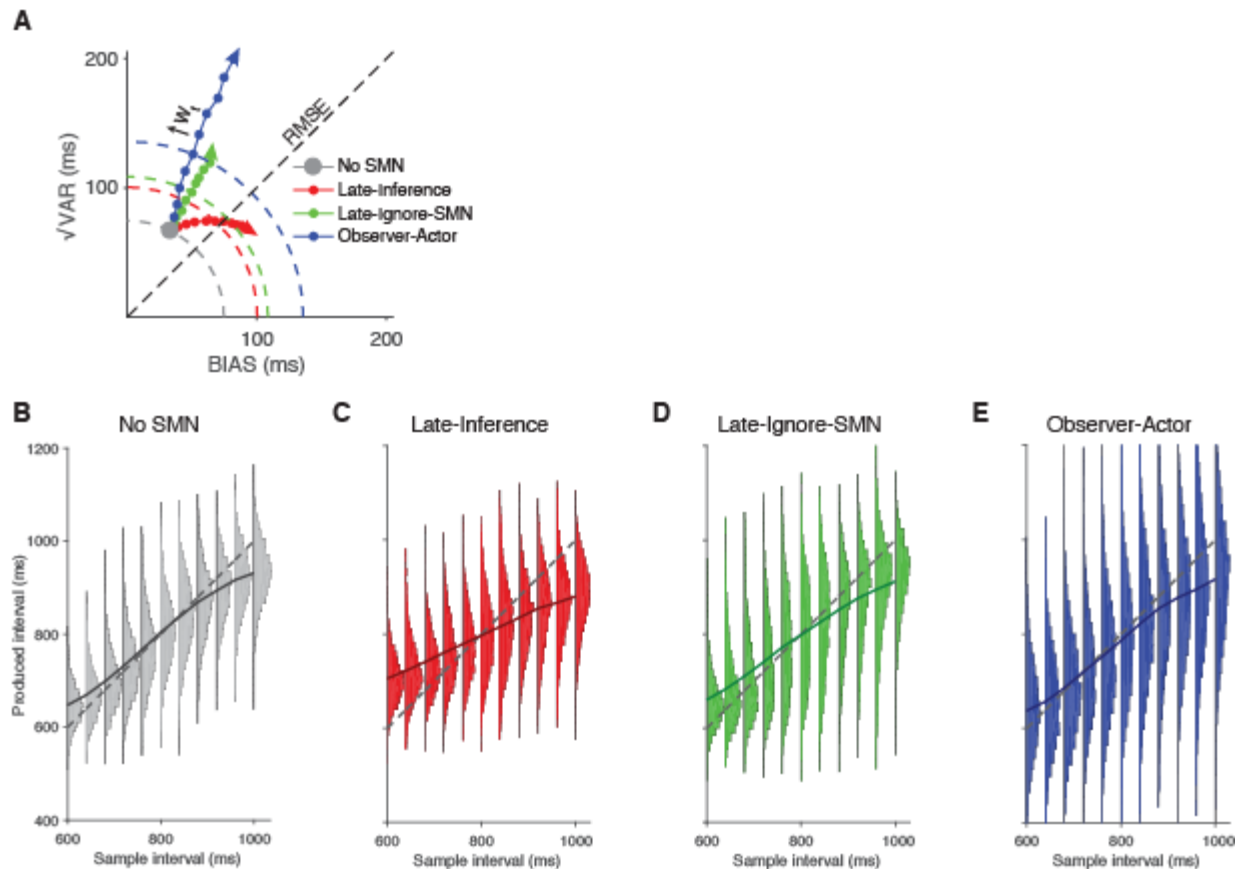
777
778
779 Here t_i is the optimal value that the observer using early inference should aim to produce in order to
780 mitigate the effects of post-inference transformation and production scalar variability. Like the Late-
781 Ignore-SMN model, this model was able to accommodate a slight increase in bias as it specified all
782 aimed magnitudes to be smaller than dictated by the Early-Inference model. However, also similar to
783 the Late-Ignore-SMN model, increasing SMN (w_t) primarily affected variance rather than bias
784 **(Supplemental Figure 3)**.



785
786 **Supplementary Figure 1.** Illustration of the Bayesian observer model previously shown to capture the
787 behavior of human subjects in the identity context of the timing task (Jazayeri and Shadlen 2010). The
788 noisy measurement stage (left), takes a sample interval (t_s) as input and produces a measurement (t_m)
789 corrupted by Gaussian noise with standard deviation equal to the measurement Weber fraction (w_m)
790 times the value of t_s . A deterministic Bayesian inference stage (middle) then takes t_m as input and
791 produces an inference t_i using knowledge of the prior distribution over t_s as well as the value of w_m
792 such that the the root mean squared error (RMSE) of t_i relative to t_s is minimized. Finally the noisy
793 production stage (right) takes t_i as input and generates a produced time (t_p) corrupted by Gaussian
794 noise with standard deviation equal to the production Weber fraction (w_p) times the value of t_i . This
795 model captures high response variability by increases in w_p and large response biases towards the
796 mean of the prior by increases in w_m (**Supplementary Figure 2**).



797
798 **Supplementary Figure 2.** Illustration of the effects of increasing the amount of production and
799 measurement noise. Using the Bayesian observer model (Jazayeri and Shadlen 2010), we simulated
800 the effects of varying the amount of motor production noise (green; w_p : production Weber fraction) and
801 sensory measurement noise (blue: w_m : measurement Weber fraction) on \sqrt{VAR} and *BIAS*. Increasing
802 the value of w_p substantially increased variability with almost no increase in bias, whereas increasing
803 w_m increased bias due to increased reliance on prior information, but had little effect on variability.
804 Thus, we interpret increases in w_m (**Figures 3 & 6**) for subjects in the remapped contexts as evidence
805 for reliance on prior information in a late inference strategy to mitigate the effects of increased SMN
806 relative to the identity contexts.



807

808 **Supplementary Figure 3.** Behavior of different models as a result of increasing SMN. **A.** Bias

809 variance curves for three models with increasing SMN ($w_t = 0.025 - 0.25$) relative to a “no SMN”

810 observer model (large gray circle; $w_m = 0.08$; $w_p = 0.06$). For each model (Late-Inference, red; Late-

811 Ignore-SMN, green; Observer-Actor, blue) increasing SMN (w_t) causes *RMSE* to increase as evident

812 by increasing distance of circles from the origin. The Late-Inference model compensates for increasing

813 SMN by systematic increases in *BIAS* and has the best performance. The other models exhibit less

814 *BIAS* and more \sqrt{VAR} leading to larger *RMSE* compared to the Late-Inference model. Quarter circles

815 represent combinations of \sqrt{VAR} and *BIAS* with equal *RMSE* for $w_t = 0.14$. **B-D.** Distribution of

816 responses as a function of sample duration under various models for $w_t = 0.14$. **B.** The no SMN

817 observer model, which shows the lowest *RMSE*. **C.** The Late-Inference model (red). In this model, bias

818 increases substantially while variability remains relatively stable (similar to the effect of increasing w_m ;

819 **Supplementary Figure 2**). **D.** The Late-Ignore-SMN model also adds bias; however, it also leads to a

820 comparable increase in variance. **E.** Increasing transformation noise in the Observer-Actor model

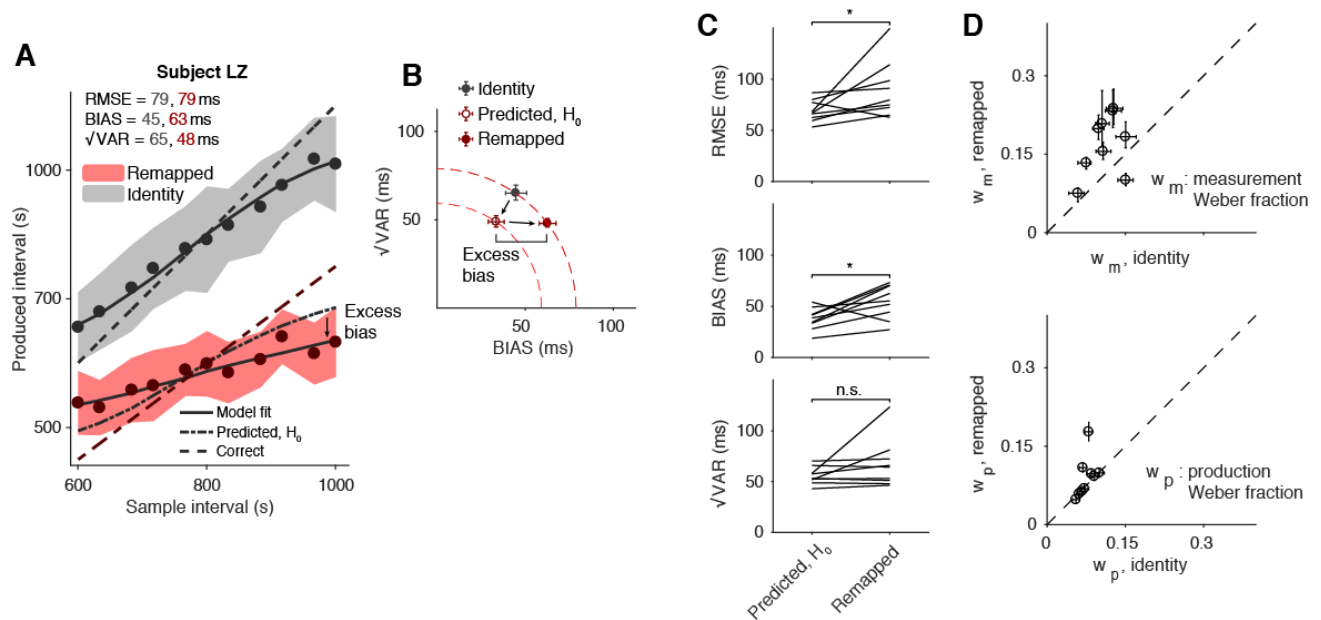
821 primarily increases variance but also adds a small amount of bias towards earlier responses. Due to

822 scalar variability, smaller response magnitudes result in lower production variability. This figure depicts

823 data simulated for the identity context; although we could not measure SMN in the identity context

824 directly, we presume that SMN exists for all behaviors involving a sensorimotor transformation (see

825 **Discussion**).



826
 827 **Supplementary Figure 4.** Time interval reproduction, gain = 0.75. An alternative explanation for
 828 increased bias in the remapped context (gain = 1.5) which does not involve late inference is that
 829 subjects did not follow task instructions, adding a constant duration to their responses rather than
 830 multiplying. To investigate this possibility, we designed a control experiment in which the gain factor
 831 was 0.75 rather than 1.5. In this case, if subjects added a constant (negative) offset, *BIAS* and fit w_m
 832 values should decrease. **A.** Performance of an example subject in the identity (gray) and remapped
 833 (red) contexts. Filled circles and shaded regions indicate mean response times \pm one standard
 834 deviation; dashed lines represent correct intervals. Solid lines represent the mean responses of a
 835 Bayesian observer model (see Methods) fit to the subject's data separately for the two contexts; the
 836 dash-dot line in the $g = 0.75$ context represents the model's behavior using parameters fit from the
 837 identity context. This simulation corresponds to the null prediction of no additional SMN in the
 838 remapped context. As was the case for $g = 1.5$, excess bias towards the mean in the remapped relative
 839 to the identity context is apparent. **B.** $\sqrt{\text{VAR}}$ vs. *BIAS* for the two contexts (gray for identity, and dark red
 840 for remapped), as well as the prediction for the remapped context assuming no additional SMN (empty
 841 circle). This prediction underestimates *RMSE* indicating larger SMN for the remapped context. The
 842 increased *RMSE* was entirely due to an increase in *BIAS* ("excess bias"). Dashed quarter circles
 843 illustrate combinations of *BIAS* vs. $\sqrt{\text{VAR}}$ giving rise to equal *RMSE*; error bars are computed from the
 844 standard deviation of bootstrapped estimates ($n = 1000$). **C.** Comparison of *RMSE*, *BIAS*, and $\sqrt{\text{VAR}}$ for
 845 nine subjects. On the left are values predicted in the remapped context (i.e. multiplied by the gain of
 846 0.75), and on the right are the actual values observed from behavior in the remapped context (*: $p <$
 847 0.05). **D.** Parameters of observer model fits. We fit the an observer model with data of individual
 848 subjects independently for the two contexts. Error bars represent 95% confidence intervals estimated
 849 using a bootstrap procedure ($n = 1000$). The results of this experiment suggest that response shifting
 850 strategy does not account for increased bias in the remapped contexts in the timing task.
 851

852 **Supplementary references**

- 853 Acerbi, Luigi, Daniel M. Wolpert, and Sethu Vijayakumar. 2012. "Internal Representations of Temporal
854 Statistics and Feedback Calibrate Motor-Sensory Interval Timing." *PLoS Computational Biology* 8
855 (11): e1002771. doi:10.1371/journal.pcbi.1002771.
- 856 Cicchini, Guido Marco, Roberto Arrighi, Luca Cecchetti, Marco Giusti, and David C. Burr. 2012.
857 "Optimal Encoding of Interval Timing in Expert Percussionists." *The Journal of Neuroscience: The*
858 *Official Journal of the Society for Neuroscience* 32 (3): 1056–60. doi:10.1523/JNEUROSCI.3411-
859 11.2012.
- 860 Jazayeri, Mehrdad, and Michael N. Shadlen. 2010. "Temporal Context Calibrates Interval Timing."
861 *Nature Neuroscience* 13 (8). Nature Publishing Group: 1020–26. doi:10.1038/nn.2590.
- 862 Landy, Michael S., Julia Trommershäuser, and Nathaniel D. Daw. 2012. "Dynamic Estimation of Task-
863 Relevant Variance in Movement under Risk." *The Journal of Neuroscience: The Official Journal of*
864 *the Society for Neuroscience* 32 (37): 12702–11. doi:10.1523/JNEUROSCI.6160-11.2012.
- 865 Trommershäuser, Julia, Sergei Gepshtein, Laurence T. Maloney, Michael S. Landy, and Martin S.
866 Banks. 2005. "Optimal Compensation for Changes in Task-Relevant Movement Variability." *The*
867 *Journal of Neuroscience: The Official Journal of the Society for Neuroscience* 25 (31): 7169–78.
868 doi:10.1523/JNEUROSCI.1906-05.2005.

Subject	Identity context						No additional SMN prediction			Remapped context					
	RMSE	BIAS	$\sqrt{\text{VAR}}$	w_m	w_p	offset	RMSE	BIAS	$\sqrt{\text{VAR}}$	RMSE	BIAS	$\sqrt{\text{VAR}}$	w_m	w_p	offset
CK	71	37	57	0.08	0.06	20	106	56	86	136	86	94	0.12	0.05	32
JM	103	72	71	0.15	0.07	-22	154	108	106	140	78	108	0.11	0.07	-32
MW	89	56	69	0.13	0.07	-1	134	84	104	171	128	112	0.21	0.07	-12
RA	91	46	78	0.11	0.08	-8	136	69	116	212	151	130	0.30	0.11	-54
SMP	83	25	77	0.06	0.08	-18	125	38	115	196	121	146	0.18	0.11	-31
LZ	79	45	65	0.10	0.06	-6	119	67	98	178	137	112	0.24	0.08	-13
DS	116	66	94	0.15	0.10	-16	173	98	140	202	136	147	0.23	0.11	-21
BG	88	52	70	0.11	0.07	15	132	77	105	191	151	114	0.29	0.09	-25

869
870 **Supplementary Table 1.** Subject performance and observer model parameters for the timing task in the identity and remapped contexts,
871 along with performance predicted for the remapped context under the prediction of no additional SMN. All values are expressed in
872 milliseconds, except for w_m and w_p , which are unitless.

873
874

Subject	Equal-SMN			Early-Inference				Late-Inference				Late-Ignore-SMN				Observer-Actor			
	w_m	w_p	BIC	w_m	w_p	w_t	BIC	w_m	w_p	w_t	BIC	w_m	w_p	w_t	BIC	w_m	w_p	w_t	BIC
CK	0.10	0.06	-2673	0.10	0.05	0.02	-2667	0.08	0.05	0.09	-2705	0.10	0.06	0.00	-2666	0.10	0.05	0.02	-2669
JM	0.13	0.07	-2317	0.13	0.07	0.03	-2312	0.13	0.07	0.00	-2310	0.13	0.07	0.00	-2310	0.13	0.07	0.03	-2312
MW	0.16	0.07	-2265	0.16	0.07	0.00	-2258	0.13	0.07	0.16	-2308	0.16	0.07	0.00	-2258	0.16	0.07	0.00	-2259
RA	0.17	0.09	-1850	0.16	0.08	0.06	-1852	0.10	0.09	0.25	-1958	0.16	0.09	0.10	-1847	0.16	0.08	0.06	-1855
SMP	0.12	0.10	-1778	0.10	0.08	0.08	-1802	0.05	0.10	0.17	-1915	0.09	0.09	0.13	-1812	0.10	0.08	0.09	-1807
LZ	0.15	0.07	-2237	0.15	0.07	0.05	-2237	0.10	0.07	0.20	-2362	0.15	0.07	0.02	-2230	0.15	0.07	0.05	-2240
DS	0.18	0.11	-1655	0.18	0.10	0.04	-1649	0.15	0.11	0.16	-1663	0.18	0.10	0.09	-1649	0.18	0.10	0.04	-1650
BG	0.17	0.08	-2094	0.16	0.08	0.04	-2089	0.11	0.08	0.24	-2206	0.17	0.08	0.00	-2087	0.16	0.08	0.04	-2092
Total			-16803				-16783				-17344				-16776				-16800

875
876 **Supplementary Table 2.** Fit parameters for the five models in the timing task. All values are unitless.

Subject	Identity context							No additional SMN prediction			Remapped context						
	RMSE	BIAS	$\sqrt{\text{VAR}}$	w_m	w_p	σ_p	offset	RMSE	BIAS	$\sqrt{\text{VAR}}$	RMSE	BIAS	$\sqrt{\text{VAR}}$	w_m	w_p	σ_p	offset
EG	0.94	0.13	0.93	0.00	0.07	0.00	0.17	1.38	0.15	1.38	1.60	0.52	1.51	0.06	0.06	0.66	-0.24
IG	1.77	0.51	1.69	0.08	0.06	1.30	1.15	2.13	0.77	1.99	2.63	1.23	2.32	0.12	0.11	0.00	-0.44
JK	1.38	0.35	1.33	0.06	0.06	0.89	0.90	1.77	0.52	1.69	1.84	0.86	1.62	0.09	0.01	1.28	-0.29
RC	1.28	0.24	1.25	0.04	0.06	0.90	0.69	1.58	0.35	1.54	1.79	0.83	1.58	0.08	0.07	0.00	-0.27
DS	1.43	0.49	1.35	0.07	0.06	0.91	0.56	1.88	0.72	1.73	2.34	0.76	2.21	0.08	0.10	0.56	-0.33
SMP	1.75	0.57	1.65	0.07	0.01	1.55	0.59	1.97	0.75	1.82	2.33	0.99	2.11	0.09	0.00	1.85	-0.22
TT	0.62	0.07	0.62	0.00	0.05	0.17	-0.10	0.92	0.10	0.91	1.62	0.31	1.59	0.03	0.08	0.00	-0.22

877

878

Supplementary Table 3. Subject performance and observer model parameters for the length task in the identity and remapped contexts,

879

along with performance predicted for the remapped context under the prediction of no additional SMN. All values are expressed in degrees

880

visual angle, except for w_m and w_p , which are unitless.

881

882

Subject	Equal-SMN				Early-Inference					Late-Inference					Late-Ignore-SMN					Observer-Actor				
	w_m	w_p	σ_p	BIC	w_m	w_p	σ_p	w_t	BIC	w_m	w_p	σ_p	w_t	BIC	w_m	w_p	σ_p	w_t	BIC	w_m	w_p	σ_p	w_t	BIC
EG	0.03	0.07	0.00	5720	0.02	0.07	0.00	0.16	5905	0.00	0.07	0.32	0.06	5608	0.01	0.07	0.34	0.06	5695	0.02	0.06	0.39	0.21	5883
IG	0.10	0.10	0.66	4988	0.09	0.10	0.83	0.15	5154	0.08	0.10	0.77	0.09	4983	0.09	0.09	1.00	0.09	4993	0.09	0.08	1.03	0.23	5152
JK	0.07	0.04	1.08	6485	0.07	0.04	1.08	0.08	6728	0.06	0.03	1.15	0.06	6474	0.07	0.04	1.08	0.00	6492	0.06	0.02	1.18	0.17	6724
RC	0.06	0.05	0.88	6287	0.06	0.06	0.85	0.00	6529	0.04	0.04	1.01	0.07	6253	0.06	0.05	0.88	0.00	6294	0.05	0.04	0.96	0.14	6527
DS	0.08	0.10	0.00	6967	0.07	0.07	0.78	0.30	7199	0.07	0.10	0.00	0.03	6974	0.07	0.10	0.17	0.07	6968	0.06	0.08	0.73	0.29	7201
SMP	0.09	0.07	1.33	4880	0.07	0.00	1.56	0.26	5036	0.07	0.06	1.37	0.06	4883	0.08	0.06	1.40	0.04	4887	0.07	0.00	1.56	0.28	5033
TT	0.00	0.07	0.00	5163	0.02	0.05	0.00	0.29	5224	0.00	0.06	0.00	0.05	5077	0.01	0.05	0.01	0.07	5054	0.01	0.05	0.01	0.29	5204
Total				40559					41857					40334					40466					41805

883

884

Supplementary Table 4. Fit parameters the for five models in the length task. All values are unitless except σ_p , which is in units of visual

885

degrees.